Quaternary Science Reviews 250 (2020) 106634

Contents lists available at ScienceDirect

Quaternary Science Reviews

journal homepage: www.elsevier.com/locate/quascirev

Complexity and asynchrony of climatic drivers and environmental responses during the Last Glacial-Interglacial Transition (LGIT) in north-west Europe

Ashley M. Abrook [a, *], Ian P. Matthews [a], Ian Candy [a], Adrian P. Palmer [a], Chris P. Francis [a], Lucy Turner [a], Stephen J. Brooks [b], Angela E. Self [b], Alice M. Milner [a]

[a] Centre for Quaternary Research, Royal Holloway University of London, Egham, Surrey, TW20 0EX, UK
[b] Department of Life Sciences, Natural History Museum, Cromwell Road, London, SW7 5BD, UK

ARTICLE INFO

Article history:
Received 15 June 2020
Received in revised form
28 September 2020
Accepted 29 September 2020
Available online 28 October 2020

Keywords:
Abrupt climate change
Vegetation
Fire
Thresholds
Event phasing
Hydrology

ABSTRACT

The Last Glacial-Interglacial Transition (*ca* 16–8 ka BP) in north-west Europe is an important period of climatic change where millennial-scale climatic evolution led to environmental reorganisation. Imprinted upon these long-term changes are a series of short-lived, centennial-scale events that appear to be spatially and temporally complex across Europe. The complexity of environmental change in response to these climatic events is poorly understood because of a paucity of paired investigations that provide evidence of both driver and response variables. We present a high-resolution palynological, charcoal and stable isotopic record alongside chironomid-inferred temperature data from Tirinie, south-east Grampian Highlands, Scotland. The record is stratigraphically and chronologically constrained using tephra and radiocarbon dating. The isotopic and chironomid data reveal centennial-scale climatic deteriorations at *ca* 14.0; 13.2 and 11.4 cal ka BP. In response to these cooling events, vegetation became more open, fire frequency increased and landscape erosion was common. The reconstruction of both climate and environment reveals asynchrony in the phasing of annual and summer temperature variability, vegetation change and fire for each climatic event. Whilst responses appear strongest following the convergence of annual and summer temperature variability across all events, the *ca* 13.2 ka BP event reveals a two-stage environmental and fire response to climatic change, and the *ca* 11.4 ka BP event exhibits environmental change in the absence of summer temperature variability. The data further suggests that fire is an integral component of abrupt climatic change in this part of north-west Europe.

1. Introduction

The identification of abrupt climatic events (ACEs) in late Quaternary records (e.g. Björck et al., 1998; Lowe et al., 2008) has led to an increased understanding of the magnitude and rapidity of climatic shifts (Steffensen et al., 2008; Rasmussen et al., 2014). One period which is characterised by abrupt climatic change at the millennial- and centennial-scale is the Last Glacial-Interglacial Transition (LGIT; 16-8 ka BP; Rasmussen et al., 2014). The LGIT represents an ideal period to investigate the structure of abrupt events across Europe due to the abundance of stratigraphically-expanded sedimentary sequences. Within the LGIT, millennial-scale climatic development is associated with warm climates of the Windermere Interstadial/Bølling-Allerød/Greenland Interstadial 1; cold climates of the Loch Lomond Stadial/Younger Dryas/Greenland Stadial 1; and climatic amelioration during the early Holocene. Additionally, centennial-scale climatic oscillations can be identified through phases of isotopic depletion within terrestrial carbonates and declines in chironomid-inferred summer temperature (e.g. Lotter et al., 1992; Brooks and Birks, 2000; Marshall et al., 2002). When such events are observed in terrestrial archives they are frequently assumed to be broadly contemporaneous with abrupt events in the NGRIP Greenland ice-core record, termed GI-1d (14.08–13.94 ka b2k), GI-1b (13.31–13.1 ka b2k) and the 11.4 ka BP event in the early Holocene (Rasmussen et al., 2007, 2014).

In north-west Europe, a number of studies demonstrate centennial-scale climatic variability with variable magnitudes of change (e.g. Lotter et al., 1992; von Grafenstein et al., 1999; Brooks

* Corresponding author.
E-mail address: ash.abrook@rhul.ac.uk (A.M. Abrook).

https://doi.org/10.1016/j.quascirev.2020.106634

and Birks, 2000; Schwander et al., 2000; Marshall et al., 2002; Heiri et al., 2007; Lang et al., 2010; Brooks et al., 2012; van Asch et al., 2012; Brooks and Langdon, 2014). However, few of these studies provide quantified evidence of climatic variation alongside palaeovegetation and/or palaeofire responses (e.g. Heiri et al., 2007; van Asch and Hoek, 2012; Turner et al., 2015; Whittington et al., 2015), therefore the sequencing and phasing of environmental responses to ACEs is still poorly understood. This complexity is compounded by 1) the lack of temporal resolution attained by many studies; 2) multi-proxy investigations from the same site performed on different sediment core sequences extracted years apart and subsequently correlated; 3) issues with proxy sensitivity and taphonomy; and 4) a lack of robust chronology. Consequently, the relationship between climate and environment requires further attention.

In this study we present the litho-, bio- (pollen and chironomids), isotopic and charcoal stratigraphy from the LGIT sediments of Tirinie, south-east Grampian Highlands, Scotland. We use a high-resolution multi-proxy approach to reconstruct millennial- and centennial-scale climatic change and to disentangle evidence of landscape response. The approach of this study also enables us to assess the role of fire in LGIT landscapes of north-west Europe and to understand the anatomy of ACEs in unprecedented detail for terrestrial contexts.

2. Site context

Tirinie (NN 886681; 56°47′17.77″ N, 34°84′47.2″ W) is a palaeolake basin located within Glen Fender, Perthshire, at the south-west fringes of the Cairngorm National Park and approximately 13 km to the north-west of Pitlochry, Scotland (Fig. 1). The site lies within a topographic low in the Schiehallion Quartzite formation, is flanked by the Blair Atholl Dark Limestone and Dark Schist formations and has a maximum extent of 0.12 × 0.05 km at an altitude of 323 m a.s.l. (Candy et al., 2016). In its present configuration the basin is an active floating bog. The site currently has a series of inflows; the most prominent being a natural spring focussed from the north-east with secondary streams draining the Meall Gruaim hillslope directly to the north. The major outflow drains the site from its western edge towards the south-west.

Original investigations at Tirinie lead to the recovery of a 420 cm sediment sequence which contained a classically tripartite sedimentological structure (Lowe and Walker, 1977). Both the tripartite structure, which at this location exhibits calcium carbonate and clastic sedimentation, alongside a typical palynological succession suggested that the sequence could be placed within the context of the LGIT. Further, variability in sedimentology and palynology at centennial-scales was noted by Lowe and Walker (1977) although not fully explored. These observations have subsequently been reaffirmed by Candy et al. (2016) with the extraction of a new sediment sequence and the identification and chemical characterisation of two discrete tephra horizons common to LGIT sediments: the Penifiler Tephra and the Vedde Ash (Turney et al., 1997; Matthews et al., 2011; Timms et al., 2019). These data, alongside depletions in stable oxygen isotopic data, suggested centennial-scale climatic variability during the Windermere Interstadial (Candy et al., 2016). However, this study did not test whether this variability could be identified across multiple climatic parameters and within different chrono- and climatostratigraphic phases.

3. Methodology

3.1. Fieldwork and lithostratigraphy

The core sequence presented here is the same core sequence presented by Candy et al. (2016). For a comprehensive review of sediment extraction and sedimentological methods readers are directed to Candy et al. (2016). For completeness, sedimentological methods include sediment description, calcium carbonate estimation using a Bascomb Calcimeter (e.g. Candy et al., 2016) and Total Organic Carbon (TOC) analysis using the Walkley-Black titration method (Schumacher, 2002). The composite record from Tirinie is represented by a 357 cm long sedimentary profile. All analyses are performed on one composite profile, with the exception of chironomid samples from the base of the sequence. Owing to a lack of material, the basal 10 chironomid samples were extracted from a duplicate core, tied to the original profile using key sedimentological marker horizons.

3.2. Palynology

The sequence was sampled for pollen between 355 cm and 198 cm at a stratigraphic resolution higher or equal to 4 cm. Through key sedimentological phases a 1 cm contiguous resolution was adopted. In total 113 pollen samples were analysed. Pollen preparation followed standard procedures outlined in Fægri and Iversen (1989) and Moore et al. (1991), including the addition of *Lycopodium* for the estimation of pollen concentrations. Density separation using sodium polytungstate (specific gravity of 2.0 g cm^{-3}) was preferred over hydrofluoric acid to separate organic and clastic sediments. Palynomorph residues were mounted using glycerine jelly. A minimum count sum of 300 Total Land Pollen (TLP) was obtained for all levels barring 354.5 to 347.5 cm and 323.5 cm to 296.5 cm where a combination of poor pollen preservation and a lack of palynomorph materials resulted in a pollen sum of 100 TLP. Pollen identification was undertaken using an Olympus CX41 binocular microscope at 400× magnification with critical identifications conducted at 1000× magnification. Moore et al. (1991) and Reille (1992) were consulted for pollen identifications with pollen nomenclature updated to reflect the botanical taxonomy of Stace (2010). All stratigraphic diagram production was performed within 'C2' V. 1.7.7 (Juggins, 2016).

3.3. Palynological data analysis

Pollen zonation was performed based on visual assessments supported by CONISS (Grimm, 1987). Principal Curves (PrC) were constructed to summarise compositional turnover in the pollen, spore and *Pediastrum* dataset. PrCs were constructed using both Correspondence Analysis (CA) and Principal Components Analysis (PCA) axis one scores as the starting curve for each PrC following the method of Simpson and Birks (2012) outlined in Abrook et al. (2020). The final PrC was fitted via regression and iteratively generated using smoothing splines with a PCA-based starting curve. The PCA method was chosen owing to model convergence in fewer iterations despite similar variances being explained by the two approaches. The PrC approach is justified here as it assists in the identification of short phases of palynological variability (e.g. Abrook et al., 2020). The PrC output is presented as a stratigraphic plot alongside the palynological data. All numerical analyses were performed using the computer programming software 'R' and the 'Rioja', 'Vegan' and 'Analogue' packages (Juggins, 2017; Oksanen et al., 2019; Simpson and Oksanen, 2019).

3.4. Charcoal analysis

Micro- and macro-charcoal analyses were performed matching the resolution of the palynological record. Micro-charcoal was extracted alongside palynological analysis, with all black, opaque, angular fragments greater than 5 μm counted on pollen slides. For

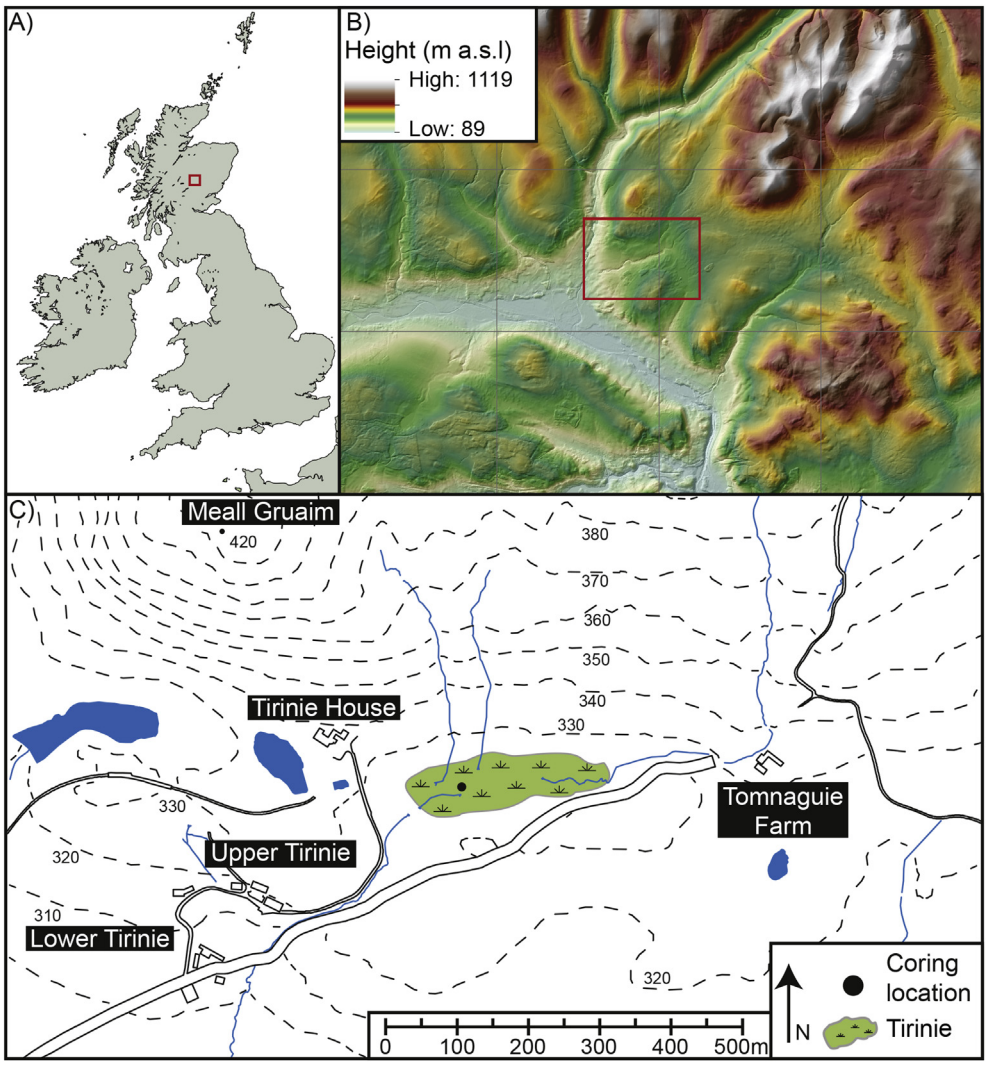

Fig. 1. Location of the Tirinie site. A) Location with respect to rest of the British Isles; B) hillshade model of the south-west Grampian Highlands; and C) topographic map of Tirinie.

macro-charcoal analyses, 1 cm^3 of sediment was extracted following procedures within Carcaillet et al. (2007). All macro-charcoal is designated as greater than 125 μm without further size differentiation and is presented as charcoal fragments cm^{-3}.

3.5. Chironomid analysis

Between 357 cm and 264 cm, samples were extracted for chironomid analysis. The resolution attained was variable; 8 cm increasing to 1–2 cm over key stratigraphic phases. A total of 34 samples were analysed for chironomids. Sample processing followed standard procedures outlined in Brooks et al. (2007) using warm 10% potassium hydroxide with head capsules picked under a Motic SMZ-168-BP stereo microscope at 25× magnification. Head capsules were mounted using Hydromatrix. Fossil chironomid head capsules were identified using a binocular CX41 microscope at 400× magnification, referencing Wiederholm (1983), Rieradevall and Brooks (2001), Brooks et al. (2007) and the chironomid reference collection at the Natural History Museum, London. Whilst a minimum count of 50 head capsules should be selected for analyses (Heiri and Lotter, 2001) this was not always possible due to a lack of head capsules preserved within the sediments. Eight samples fell below this cut off at 356.5, 354.5, 329.5, 326.5, 288.5, 277.5, 273.5 and 264.5 cm. Analyses were still performed on these samples, however the data carries caveats regarding reliability.

3.6. Chironomid-inferred temperature reconstruction

Mean July air temperature estimates were obtained from the square-root transformed fossil chironomid percentage abundance data using both the modern Norwegian and the combined Swiss-Norwegian chironomid temperature calibration datasets. The modern Norwegian calibration set was ultimately selected for the temperature reconstruction (see Supplementary Information 1 for data comparisons and a discussion of Norwegian versus Swiss-Norwegian calibration at Tirinie). The Norwegian dataset is expanded from the previously published 109-lake calibration set (Brooks and Birks, 2001). It consists of 157 lakes, however, four outlier lakes were removed. A two-component weighted-averaging partial least squares (WA-PLS; ter Braak and Juggins, 1993) model was selected, with a root mean squared error of prediction (RMSEP) of 1.1 °C, a coefficient of determination (R^2JACK) of 0.9 and a maximum bias of 1.13 °C, estimated by leave-one-out cross-validation. Sample specific errors were calculated using 999 bootstrapping cycles with values ranging from 1.12 to 1.25 °C per sample.

Several criteria were used to assess the reliability of the mean July air temperature reconstructions. Goodness-of-fit to temperature was assessed by plotting the fossil chironomid assemblage in the CCA ordination space of the calibration dataset constrained by July temperature only. Fossil samples that had a squared residual distance value in the extreme 10% and 5% of the ordination space were considered to have a poor and very poor fit to temperature, respectively (Birks et al., 1990). The modern analogue technique tested the similarity of fossil assemblages to those found in the modern calibration dataset. Where the squared-chord distance exceeded the 5th and 10th percentiles, samples were considered to have poor and very poor modern analogues in the calibration set (Birks et al., 1990). Additionally, the percentage of taxa that are considered rare (i.e. taxa with a Hill's N2 of less than five; Heiri et al., 2003) and taxa that are absent in the modern calibration dataset should be low (Birks, 1998). Assessments of temperature reliability were made using the 'Vegan' and 'Analogue' packages in 'R' (Oksanen et al., 2019; Simpson and Oksanen, 2019).

3.7. Stable isotope analysis

Oxygen and carbon isotopic analyses ($\delta^{18}O$ and $\delta^{13}C$) have previously been performed at Tirinie between 355 and 327 cm (Candy et al., 2016). In this study the isotopic profile is extended to sediments between 291 and 198 cm, at a resolution no greater than 8 cm increasing to 1 cm where analyses showed more complex isotopic signals. All methodological approaches follow Candy et al. (2016), including wet sieving over a 63 μm mesh to separate coarse shell fractions from authigenic calcite and the use of hydrogen peroxide to remove organic material. $\delta^{18}O$ and $\delta^{13}C$ values were measured by analysing CO_2 liberated from a sample reaction with phosphoric acid at 90 °C. Internal (RHBNC-PRISM) and external (NBS-19, LSVEC) standards were run every ten samples. The carbonate stable isotopes were analysed using a VG PRISM series 2 mass spectrometer. All stable isotopic values are quoted with reference to VPDB.

3.8. Chronology

Five macro-fossil samples were prepared for radiocarbon assessment using duplicate cores tied to the master profile based on key stratigraphic marker horizons. Unfortunately, only one sample yielded sufficient carbon for measurement. To construct the age model, this sample at 334.5 cm was combined with age estimates of known tephra horizons which have been recalibrated using IntCal20. To constrain the model at the top of the sequence, the position of the *Corylus* rise was imported from Kelly et al. (2017) with the assumption that the rise in *Corylus* at Inverlair coincides with, or occurs soon after, the rise at Tirinie. Further, the date of the An Druim Tephra (Timms et al., 2019) was incorporated at the *Corylus* rise as a *Terminus Ante Quem* as the An Druim Tephra occurs after *Corylus* at Inverlair and other sites in Scotland (Kelly et al., 2017; Abrook et al., 2020).

Using these data, a *P_Sequence* depositional model was constructed using the IntCal20 calibration curve (Reimer et al., 2020) in OxCal V. 4.4.2 (Bronk Ramsey, 2008, 2009). No boundaries were added to the model over areas of lithostratigraphic variability and the k_parameter was permitted to vary over two orders of magnitude from a starting value of one.

4. Results

4.1. Lithostratigraphy

The lithostratigraphy is presented in Fig. 2 and Table 1. The recovered sequence comprises two units of calcium carbonate, interspersed by units of silt and clay. The complete sequence contains 13 units between the depths of 357-195 cm (TIR-L*n*). Units TIR-L1 to TIR-L6 exhibit variability between clastic and carbonate sedimentation with the latter containing $CaCO_3$ values between 13 and 94%. Over phases of reduced $CaCO_3$, increases in Total Organic Carbon (TOC) are noted (maximum of 14.9%). TIR-L7 exhibits a shift to clastic silt and clay sedimentation with negligible $CaCO_3$ but three distinct peaks in TOC (15.9, 15.1 and 14.0% respectively. Overlaying TIR-L7, units TIR-L8 to TIR-L12 are dominated by carbonates with $CaCO_3$ values between 61 and 99%. TIR-L13 is represented by a capping peat.

4.2. Palynology

A total of 11 local pollen assemblage zones (LPAZ; TIR-P*n*) have been identified throughout the sequence. The depths of these zones, alongside key taxa, are presented in Fig. 3 and Table 2.

TIR-P1 to TIR-P5 are dominated by fluctuating percentages of *Betula*, *Juniperus*, *Empetrum*, Poaceae, Cyperaceae, *Artermisia*, *Rumex* and *Pediastrum*. TIR-P1, TIR-P3 and TIR-P5 demonstrate increased percentages of pollen associated with woody vegetation; namely *Betula* (10 to 21% within TIR-P1 and TIR-P3a; 58 and 18% in TIR-P3b and TIR-P5 respectively); *Juniperus* (20% in TIR-P3a and peaking at 42% within TIR-P5) and *Empetrum* (19% within TIR-P1 and TIR-P3a). TIR-P2 and TIR-P4 exhibit reductions in these pollen types with increased percentages of Poaceae, Cyperaceae, *Artemisia* and *Rumex*. TIR-P2 shows increased percentages of Poaceae (from 27 to 51%), *Artemisia* (increasing to 9%) and *Rumex* (from

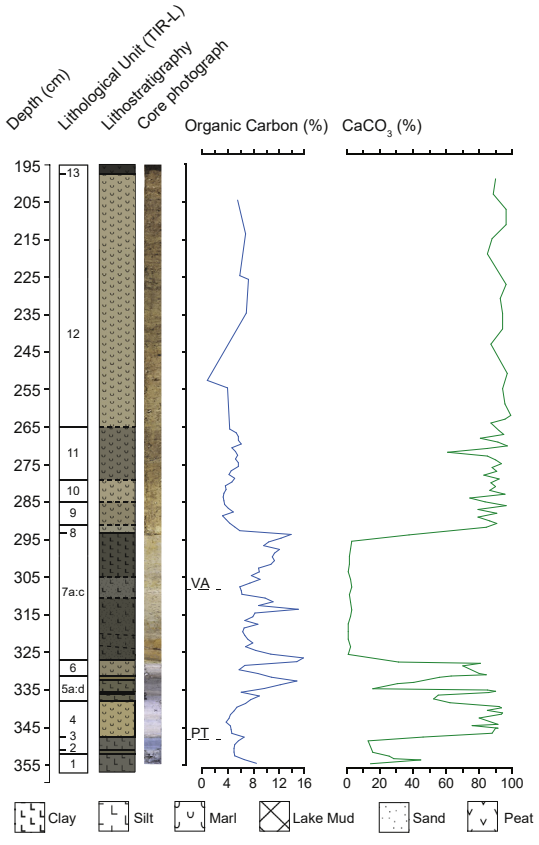

Fig. 2. Stratigraphy of the Tirinie sequence. Total Organic Carbon (TOC) values are shown alongside calcimetry data ($CaCO_3$) from the site. Also indicated are the positions of two tephra horizons: PT) Penifiler Tephra and VA) Vedde Ash (Candy et al., 2016).

Table 1
Main lithological units attributed to the Tirinie sequence.

Unit	Depth (cm)	Sediment composition	Interpretation
TIR-L13	197–195	Peat	Early Holocene
TIR-L12	265–197	Marl with shelly and detritus	
TIR-L11	279–265	Silty marl	
TIR-L10	285–279	Marl with increased shells	
TIR-L9	291–285	Marl with shells	
TIR-L8	293–291	Marl	
TIR-L7	327.5–293	Clayey sandy silt (inc. clay 305-293 cm)	Loch Lomond Stadial
TIR-L6	331–327.5	Marl	Windermere Interstadial
TIR-L5a:d	338–331	Grey clayey silt; Marl; Grey clayey silt; carbonate gyttja	
TIR-L4	347.5–338	Marl	
TIR-L3	351–347.5	Grey silty clay	
TIR-L2	352–351	Silty marl with clay	
TIR-L1	357–352	Grey silty clay	

4 to 21%). Within TIR-P4 reductions in *Betula* and *Juniperus* occur with increased Poaceae, Cyperaceae, *Rumex* and *Pediastrum* (Poaceae increases to 35%, *Rumex* to 25% and *Pediastrum* to 12%).

Within TIR-P6 woody pollen percentages are low (<12%). Percentages of Poaceae and Cyperceae are consistent and stable (largely between 15 and 25%). Whereas percentages of *Artemisia* at the zone onset are low but increase to a profile maximum towards the top of the zone (up to 33%). Percentages of *Rumex* increase towards the start of the zone then stabilise (between 15 and 20%). During this zone a substantial increase in *Pediastrum* is identified (from <5% to between 45 and 60%). Additionally, Caryophyllaceae, Lactuceae and *Saxifragaceae* are common alongside spores of *Selaginella selaginoides*.

TIR-P7 is characterised by elevated percentages of *Salix*, Poaceae, Cyperaceae, *Rumex* and *Myriophyllum*. These taxa decline by the top of the zone but continue into TIR-P8a and TIR-P8b. A spike in *Equisetum* (34 to 56%) occurs between 278.5 and 273.5 cm but reduces within TIR-P8b (between 9 and 29%). TIR-P8a and TIR-P8b exhibit subtle percentage shifts in *Betula* and *Empetrum* (with percentage falls of 13 and 5% respectively) alongside moderate percentages of Poaceae, Cyperaceae and *Rumex*. Throughout the remainder of the palynological profile, TIR-9 to TIR-P11, increasing percentages of woody pollen occur with *Juniperus* peaking in TIR-P9, *Salix* in TIR-P10 and *Betula* in TIR-P11. Throughout these zones *Filipendula* is continually present whilst many of the previously identified herbs are either not identified or exhibit low percentages (<5%). Finally, within TIR-P11 *Corylus* percentages rise.

4.2.1. Palynological data analysis

The PrC explains 88% of the variation within the palynological dataset. The gradient defined by the PrC has *Betula* woodland and Arctic/alpine herbaceous vegetation as its two end members. Across this gradient, phases of variability in the PrC are confined to a larger oscillation between 326.5 cm and 293.5 cm (TIR-P6; Fig. 3) and a further three phases of variability within the curve (labelled 1:3 in Fig. 3). These inflections occur from 351 to 348 cm (TIR-P2); 339 to 331 cm (TIR-P4) and 280 to 264.5 cm (TIR-P8). The larger oscillation and each of the shorter oscillations suggest compositional turnover in the palynological profile.

4.3. Charcoal record

Macro-charcoal counts range from 0 to 72 fragments cm^{-3}. Six phases of increased macro-charcoal abundance can be observed. These phases contain charcoal counts of 16 (TIR-P2/3a), 72 (TIR-P4), 39 (TIR-P5), 44 (TIR-P8b), 19 (TIR-P11) and 20 (TIR-P11) fragments respectively (Fig. 3). Micro-charcoal counts are not described owing to similarities with the macro-charcoal record.

4.4. Chironomid assemblages

A total of 54 chironomid taxa were identified to species or genus morphotype throughout the sequence and placed into seven assemblage zones (Fig. 4 and Table 3).

The lowest zone, TIR-C1, is dominated by cool-temperate chironomid taxa including *Microtendipes pedellus*-type and *Procladius*. TIR-C2 is dominated by the cold and ultra-cold stenothermic taxa *Micropsectra insignilobus*-type, *Tanytarsus lugens*-type and *Micropsectra radialis*-type. The temperate taxa *Procladius* is also present. Within TIR-C3 there is an increase in cool temperate taxa including *Parakiefferiella* type-A, *Cricotopus laricomalis*-type and increasing representation of *Tanytarsus glabrescens*-type. The cold taxon *Sergentia coracina*-type is also noted. TIR-C3 shows increased abundances of the temperate taxon *Dicrotendipes nervosus*-type. Whilst the assemblage is similar during TIR-C4, abundances of taxa that were high during TIR-C3 are reduced, with an increase in the cold taxon *Sergentia coracina*-type and the cool climate *Psectrocladius sordidellus*-type. Taxa common in TIR-C3 are also identified within TIR-C5.

Large changes in the profile exist within TIR-C6. All cool temperate and temperate taxa decrease in abundance and are replaced by a cold faunal assemblage consisting of *Tanytarsus lugens*-type and *Corynocera ambigua*. Other taxa include *Hydrobaenus lugubris*-type and *Sergentia coracina*-type. Within TIR-C7 the cool temperate taxa *Psectrocladius sordidellus*-type, *Procladius*, *Tanytarsus glabrescens*-type and *Microtendipes pedellus*-type occur, together with several temperate and warm taxa.

4.4.1. Temperature reconstruction

The chironomid-inferred summer temperature reconstruction (C-IT) is presented in Fig. 5. Mean July temperatures are high within TIR-C1; TIR-C3 and TIR-C5 (*ca* 13 to 11 °C; although reducing to ca 9.0 °C towards the top of TIR-C5). However, within TIR-C2 and TIR-C4 temperatures decline to 8.8 ± 1.1 °C (TIR-C_e1; 349.5 cm) and 10.1 ± 1.1 °C (TIR-C_e2; 335.5 cm) respectively. TIR-C6 exhibits the coldest temperatures throughout the record with a minimum reconstructed temperature of 7.0 ± 1.2 °C (304.5 cm). Temperatures rise during TIR-C7 with a maximum temperature of 13.7 ± 1.2 °C. These temperatures approach the modern average July temperatures of 14.8 °C.

4.5. Oxygen and carbon isotopic record

The isotopic data (Fig. 5) generated from TIR-L1 to TIR-L6 have been presented and described in Candy et al. (2016). To summarise, there is no evidence for co-variance within the $\delta^{18}O$ and $\delta^{13}C$ datasets ($R^2 = 0.13$). The $\delta^{13}C$ values at the base of the record are

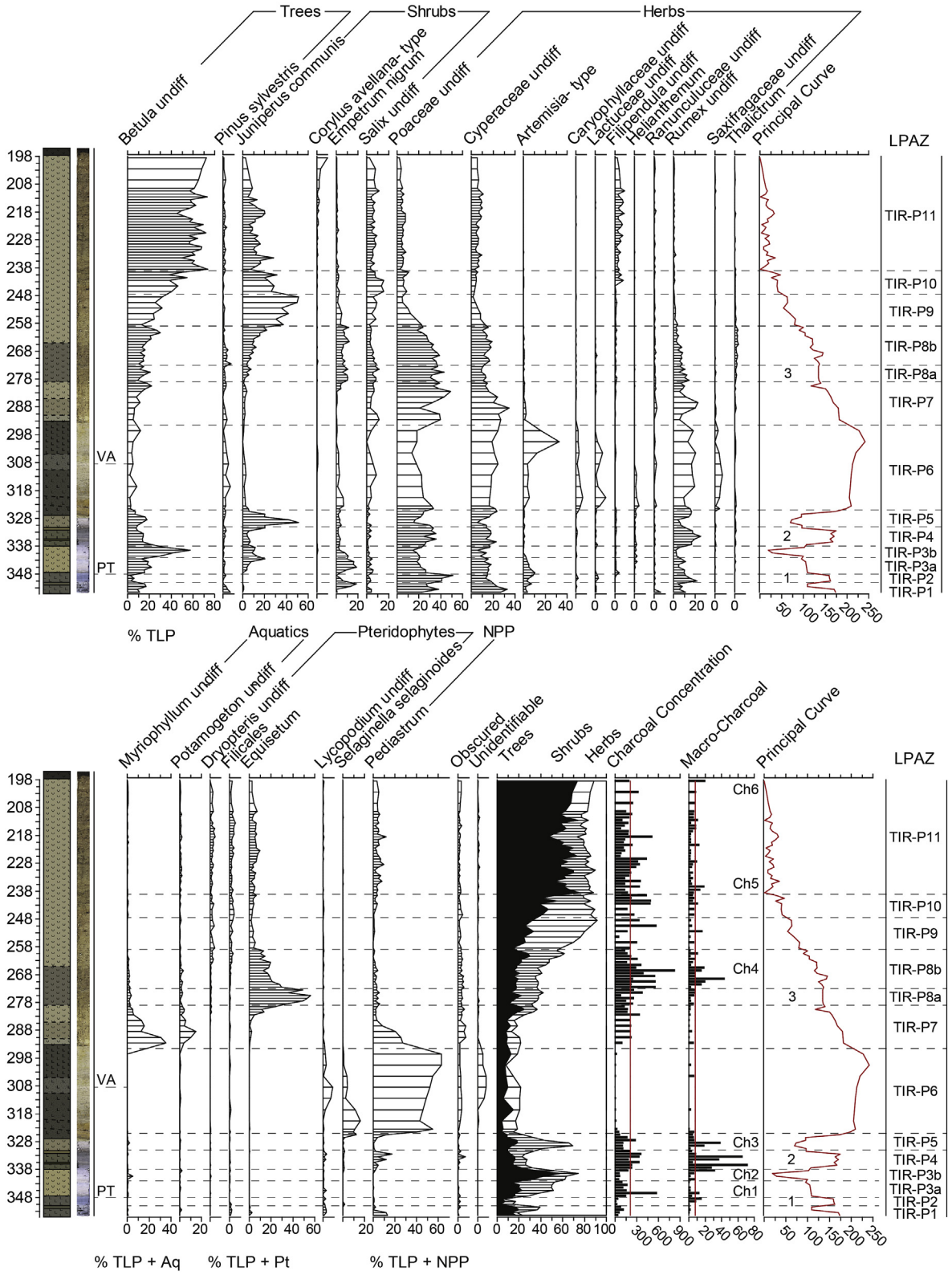

Fig. 3. Summary pollen percentage, charcoal and principal curve data from Tirinie shown against depth (cm) with local pollen assemblage zones (LPAZ). Positions of the Vedde Ash (VA) and the Penifiler Tephra (PT) have been added. Vertical red lines denote average charcoal values with labelling (Ch) showing peaks above the average. PrC numbers relate to palynologically defined events. (For interpretation of the references to colour in this figure legend, the reader is referred to the Web version of this article.)

Table 2
Main pollen assemblage zones within the Tirinie sequence.

Zone	Depth (cm)	Key taxa
TIR-P11	239–198	*Betula*
TIR-P10	247.5–239	*Betula, Juniperus*
TIR-P9	259–247.5	*Juniperus, Betula*
TIR-P8b	273–259	*Equisetum*, Poaceae, Cyperaceae
TIR-P8a	279–273	*Equisetum*, Poaceae, *Rumex*
TIR-P7	293.5–279	Poaceae, *Rumex, Myriophyllum*
TIR-P6	325–293.5	Poaceae, *Artemisia, Rumex, Selaginella, Pediastrum*
TIR-P5	331–325	*Juniperus, Betula*
TIR-P4	338–331	Poaceae, *Rumex, Pediastrum*
TIR-P3b	342–338	*Betula, Juniperus*
TIR-P3a	348–342	Poaceae, Cyperaceae, *Empetrum, Juniperus*
TIR-P2	351–348	Poaceae, *Rumex, Artemisia*
TIR-P1	355–351	Poaceae, Cyperaceae, *Empetrum*

relatively enriched (2.39‰) and follow a trend towards isotopic depletion (−3.70‰) whilst the $\delta^{18}O$ record oscillates between relatively more enriched and depleted values. Periods of depletion exhibit values of −9.03‰ (TIR-O1; 351.5 cm) and −9.35‰ (TIR-O2; 334.5 cm) (Candy et al., 2016).

Insufficient carbonate within TIR-L7 precluded any isotopic analyses. However, between TIR-L8 and TIR-L12 there is moderate evidence of co-variance ($R^2 = 0.425$). The $\delta^{13}C$ record follows the same trend of isotopic depletion (from −2.63‰ at 290.75 cm to −5.35‰ at 198.75 cm) and average $\delta^{13}C$ values are −3.60‰ ($1\sigma = 0.86$). The $\delta^{18}O$ record contains the same range of values as TIR-L1 to TIR-L6 with an average of −8.60 ($1\sigma = 0.29$). The record can be split into a phase of relative isotopic enrichment between 290.75 and 278.75 cm; a depleted phase (TIR-O3) between 281.75 and 264.75 cm and the remainder of the record where following enrichment, $\delta^{18}O$ values trend towards isotopic depletion. Within TIR-O3 $\delta^{18}O$ values deplete from −7.38‰ to −9.11‰.

4.6. Chronology

The chronological model from Tirinie produced good model agreement and has therefore been used to provide age ranges for climatic and environmental reconstructions. The age-depth model suggests that sediments were deposited in the basin from 14.27 ± 0.48 cal ka BP with the end of the studied sequence being

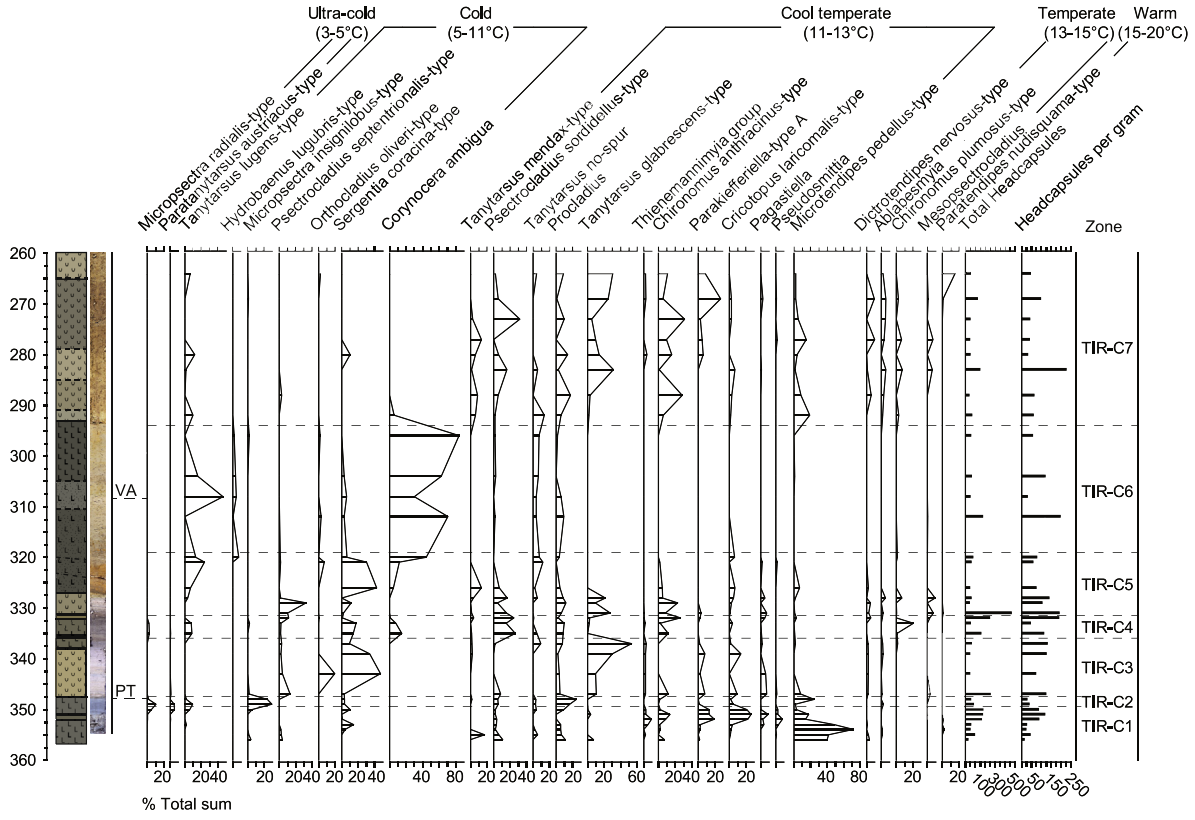

Fig. 4. Summary chironomid data from the Tirinie sequence against depth (cm). Shown are the key taxa, chironomid zones and the position of the two tephra layers (PT and VA).

Table 3
Chironomid assemblage zones from the Tirinie sequence.

Zone	Depth (cm)	Key chironomid taxa
TIR-C7	294–264	*Chironomus anthracinus*-type, *Tanytarsus glabrecens*-type, *Psectrocladius sordidellus*-type
TIR-C6	319–294	*Corynocera ambigua*, *Tanytarsus lugens*-type
TIR-C5	332–319	*Tanytarsus glabrecens*-type, *Psectrocladius septentrionalis*-type, *Sergentia coracina*-type, *Tanytarsus lugens*-type
TIR-C4	336–332	*Psectrocladius sordidellus*-type, *Chironomus anthracinus*-type, *Chironomus plumosus*-type
TIR-C3	348–336	*Sergentia coracina*-type, *Tanytarsus glabrecens*-type
TIR-C2	351–348	*Micropsectra insignilobus* type, *Micropsectra radialis*-type
TIR-C1	357–351	*Microtendipes pedellus*-type, *Parrakiefferiella* type A, *Procladius*

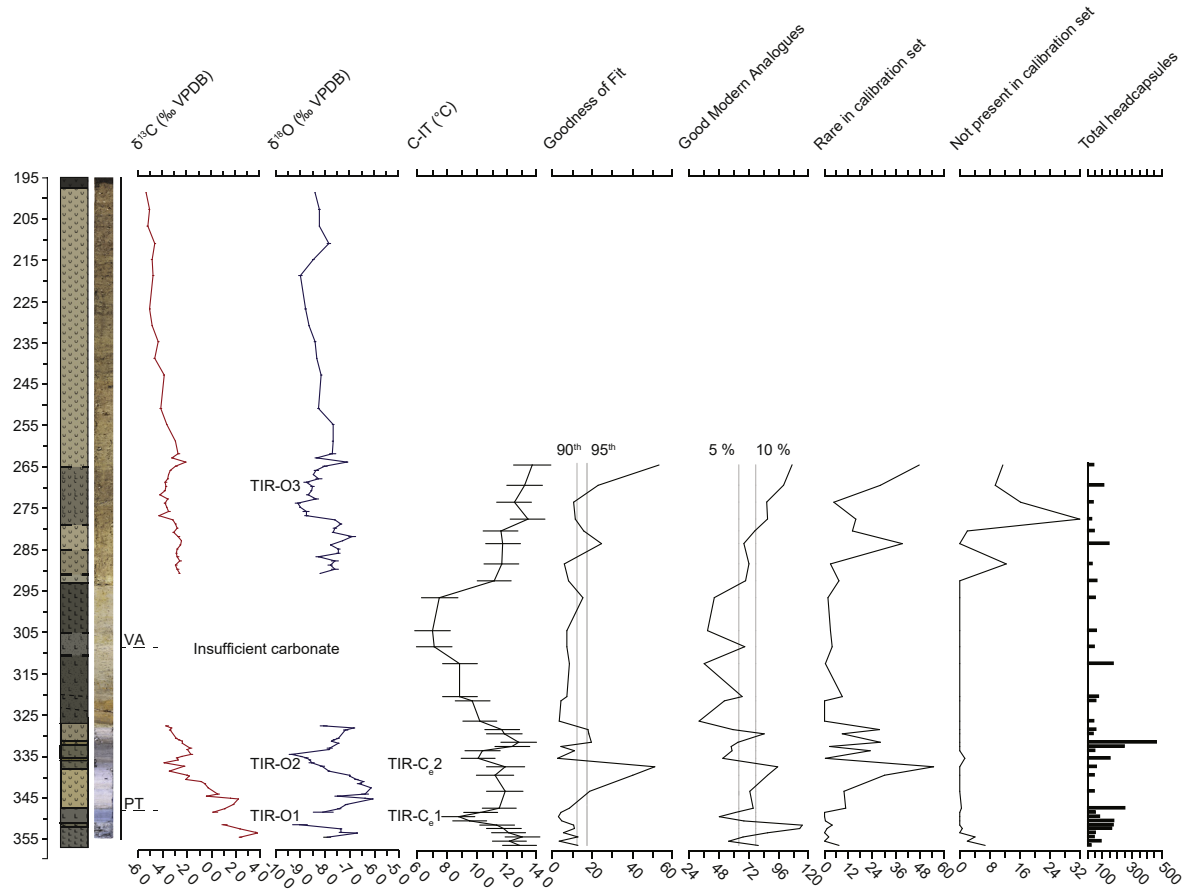

Fig. 5. Stable isotopic ($\delta^{18}O$ and $\delta^{13}C$) and chironomid-inferred temperature (C-IT) reconstruction from the Tirinie sequence. Alongside the C-IT estimates are nearest modern analogue, goodness-of-fit, percentage of rare taxa in the modern calibration set and percentage of taxa not present in modern calibration set data. 90th and 95th percentiles have been added to goodness-of-fit data and 10th and 5th percentiles to modern analogues. TIR-O (isotopes) and TIR-Ce (chironomids) relate to events in each record. Also shown are the position of the two tephra layers (PT and VA).

9.93 ± 0.6 cal ka BP (Table 4; Fig. 6).

5. Interpretation

5.1. Stratigraphy

Candy et al. (2016) argued that the Tirinie sequence spans much of the Last Glacial-Interglacial Transition (LGIT) in Scotland. This was proposed on the basis of 1) the identification of the Penifiler Tephra (e.g. Matthews et al., 2011) and the Vedde Ash (e.g. Turney et al., 1997; Lane et al., 2012); 2) the tripartite sedimentological structure; and 3) the basal pollen stratigraphy. The work presented here supports this view with the elucidation of additional palynological and chironomid-inferred mean July temperature (C-IT) variability during the LGIT (e.g. Lowe and Walker, 1977; Brooks and Birks, 2000; Brooks et al., 2012; Walker and Lowe, 2017). This study therefore builds on the framework presented by Candy et al. (2016) and places climatic and environmental variability alongside a chronology. Based on this evidence TIR-L1 to TIR-L6 is associated with the Windermere Interstadial (WI); TIR-L7 to the Loch Lomond Stadial (LLS); and TIR-L8 to TIR-L13 to the early Holocene (EH) (Table 1). Within sediments associated with the WI (TIR-L2b and TIR-L4a:d) and early Holocene (TIR-L10) there are clear sedimentological variations which appear to relate to centennial-scale climatic and landscape changes.

5.2. Validity of summer temperature reconstructions

Of all chironomid samples, 21 have a good fit to temperature (Fig. 5). However, four have a poor fit and nine have a very poor fit

Table 4
Summary of the tephra data and unmodelled input ranges used to create an age model at Tirinie. The Penifiler Tephra (adapted from Kearney et al., 2018) and Vedde Ash input ranges have been updated to IntCal20 ages. Shown are the modelled outputs (95.4% confidence interval) quoted using IntCal20.

Name	Depth (cm)	Unmodelled Range (cal BP)	Modelled range (cal ka BP	μ ± σ (This study)	Reference
Boundary	195		11,166–9184	9934 ± 600	
Before Corylus	198	9778–9564	9778–9564	9671 ± 53	Timms et al. (2017)
Before An Druim Tephra					
Vedde Ash	309	12,070–11,925	12,074–11,929	12,001 ± 36	Bronk Ramsey et al. (2015)
SUERC-78788 (*Betula* Twig)	334.5	13,167–13,087	13,168–13,089	13,125 ± 25	
Penifiler Tephra (prior)	348	14,120–13,830	14,111–13,816	13,958 ± 83	This study
Boundary	357		15,319–13,787	14,270 ± 485	

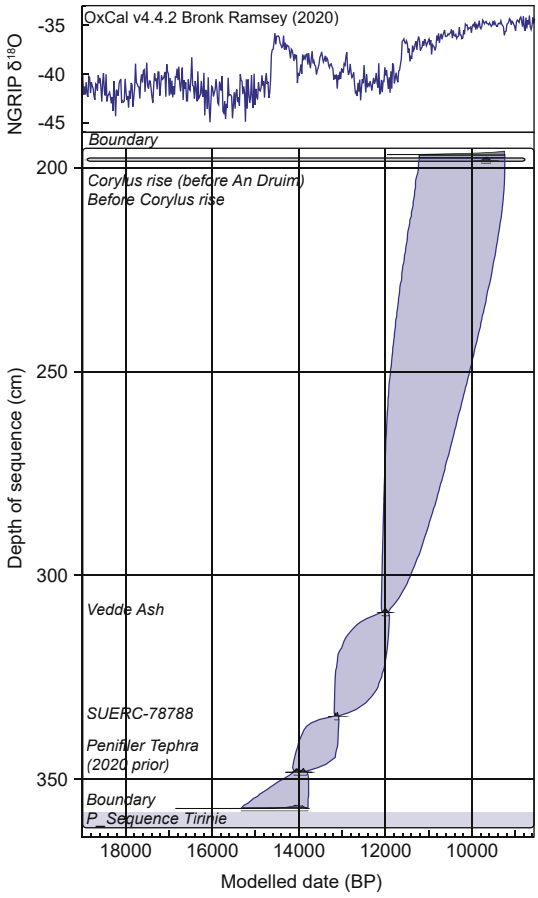

Fig. 6. Age-depth model from the Tirinie sequence with age uncertainties plotted alongside the NGRIP isotopic record. Boundaries have been added to the top and bottom of the sequence to aid in interpretations.

(see Supplementary Information 1 for comparison with the combined Swiss-Norwegian dataset). This is primarily caused by fossil samples having a high abundance of taxa rare in the modern calibration dataset. For example, *Tanytarsus glabrescens*-type (Hill's N2 3.61 in the training set) forms up to 53% of some fossil samples (339.5 and 337.5 cm). Further, five chironomid samples (288.5, 277.5, 273.5, 269.5 and 264.5 cm) have between 10% and 32% of their assemblages composed of taxa not present in the modern dataset. This is due to the presence of *Parakiefferiella*-type Swiss (Brooks and Heiri, 2013) and *Tanytarsus lactescens*-type. The exclusion of these taxa caused count sums to fall below the recommended number of 50 head capsules in two samples (354.5 and 264.5 cm) and considerably reduced sums below this value in a further two samples (277.5 and 273.5 cm). Four additional samples (356.5, 329.5, 326.5 and 288.5 cm) also fell below the recommended number of head capsules. Eleven samples have poor analogues in the modern calibration dataset (performing better than the combined dataset; Supplementary Information 1) however, WA-PLS can perform well in non-analogue situations (Birks, 1998). Whilst these statistics do not suggest that the temperature reconstructions are in-valid they do suggest additional caveats to the data. Credence from this reconstruction stems from neighbouring samples to those with poor fit to temperature, or those with reduced head capsules, having similar reconstructed temperatures. Therefore, whilst caveats exist, the reconstruction is valid.

5.3. Nature of the carbonate and oxygen isotopic signal

A complete discussion on the controls of isotopic data in lacustrine sequences is beyond the scope of this paper. However, they will be considered briefly with respect to the C-IT reconstruction. The carbonates precipitating within sediments attributed to the Windermere Interstadial (TIR-L1 to TIR-L6) are described as being a fine-grained, pure calcite mud with no ostracod tests, few mollusc shells and no chara remains (Candy et al., 2016). In comparison, the carbonates precipitating within TIR-L8 to TIR-L12, during the early Holocene, are similar albeit with a greater concentration of mollusc shells. The presence of molluscs is not thought to affect the isotopic signal, through differential fractionation with vital offsets, as shell fragments were removed during isotopic sample preparation.

Candy et al. (2016) proposed that the primary control on the $\delta^{18}O$ of the Tirinie sequence was regional air temperatures. This is often proposed as the driving factor behind oxygen isotope variability in British LGIT sequences as: 1) air temperature controls the isotopic composition of air masses and the $\delta^{18}O$ of rainfall (Rozanski et al., 1992; 1993); 2) rainfall recharges lake basins, transferring its $\delta^{18}O$ signal to groundwaters and consequently lake waters with minimal modification (Candy et al., 2016; Blockley et al., 2018); and 3) the $\delta^{18}O$ of any carbonate precipitating within a lake basin is strongly controlled by the isotopic value of lake waters (Leng and Marshall, 2004) with the addition of a temperature control during carbonate mineralisation (Kim and O'Neal, 1997). A regional air temperature control on the $\delta^{18}O$ of carbonate at Tirinie is supported by the C-IT reconstruction within this study as there is a close correspondence between shifts in $\delta^{18}O$ values and shifts in reconstructed July temperature (Figs. 5 and 7).

Whilst this is true for many of the climate events, there are shifts in $\delta^{18}O$ values that are not associated with comparable shifts in C-ITs (Section 6.2). In these cases, it is possible that variables controlling proxy variability are decoupled and the isotopes are responding to a different environmental parameter, other than summer temperature. It was argued in Candy et al. (2016) that the WI Tirinie isotopic record was unaffected by detrital contamination or intra-basin hydrological modification (i.e. evaporation; snow melt in-wash). This suggestion was supported by a lack of covariation between $\delta^{18}O$ and $\delta^{13}C$ which implies both a lack of bedrock limestone in the lake sediments and an absence of evaporation in the lake waters (Talbot, 1990). As such Candy et al. (2016) envisaged that, during the LGIT, Tirinie was an open system with rapid inflows and outflows, resulting in a constant recharge of the lake waters nullifying any potential effects of lake water isotopic modification via nivel or snow melt. In the absence of these modifying effects, other climatic parameters could explain the divergence of the two proxies. For example, it is possible that major shifts in precipitation regime may produce a recordable shift in $\delta^{18}O$ values but no associated shift in C-ITs. It is also possible that shifts in winter temperature may be recorded in the $\delta^{18}O$ of carbonate, whilst the chironomid record, which primarily reflects mean July temperatures, would not respond. This is proposed because the $\delta^{18}O$ of lake waters reflect the $\delta^{18}O$ of mean annual precipitation which has been homogenised during recharge. This is especially true of Tirinie which likely existed as a small, well-mixed lake system during the LGIT (Candy et al., 2016). Shifts in winter, summer or mean annual temperature alongside changes in the seasonality of precipitation will all, therefore, be recorded in the isotopic record, whereas C-ITs would record the summer temperature component of these changes. Consequently, an environmental shift that is seen in the $\delta^{18}O$ record, which occurs prior to or is not present within the C-IT record, may reflect climatic events that cause a strong decline in winter temperatures but only minor

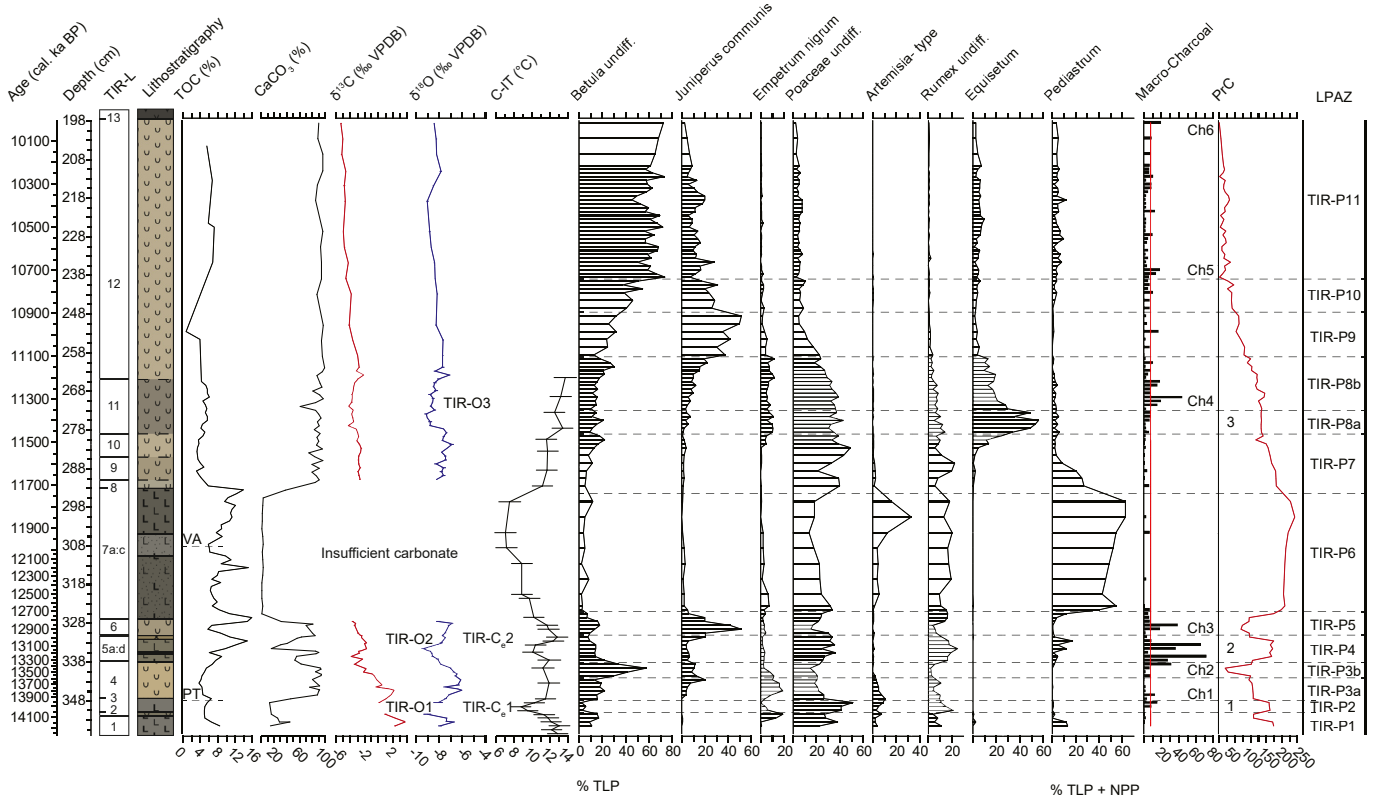

Fig. 7. Summary of all palaeodata from the Tirinie sequence plotted against age. Events in each record are labelled as TIR-O (isotopes), TIR-C_e (C-IT), Ch (charcoal) and numerical (PrC). The red vertical line denotes the average charcoal value, peaks above this are deemed important. (For interpretation of the references to colour in this figure legend, the reader is referred to the Web version of this article.)

changes in summer conditions (Section 6.2).

An additional consideration is isotopic variability at the moisture source. Changes at the moisture source relate to advection and mixing of water masses and changes in terrestrial freshwater storage. At present, it is difficult to discern whether mixing of water masses occurred over the time-period investigated by this paper. Further, whilst oceanic isotopic variability occurs over glacial/interglacial cycles, it is not thought that ice-volume changes at time-scales reported here would affect the geochemical composition of moisture sources for this location. High volume inputs of isotopically light freshwater, depending on the location, *could* influence the composition of the moisture source; however the routing of freshwater in the North Atlantic (e.g. Thornalley et al., 2010) is not thought to preferentially drive isotopic variability at the moisture source over annual or seasonal climatic variability (see Section 6.2). Equally, the close approximation of shifts in the $\delta^{18}O$ of lake carbonate and shifts in independent temperature proxies from a number of sites (van Asch et al., 2012; Blockley et al., 2018) would support the conclusion that temperature is the primary control in $\delta^{18}O$ variability. We therefore argue that in the absence of moisture source variability and intra basin hydrological modification, the Tirinie $\delta^{18}O$ record can be interpreted as reflecting an annual signal of prevailing temperature with a strong seasonal component.

5.4. Climatic evolution during the LGIT

Based on climatic and lithostratigraphic data, the WI at Tirinie extended from 14.27 ± 0.48 cal ka BP to 12.82 ± 0.29 cal ka BP (Fig. 7). The base of the record exhibits warm mean July temperatures (*ca* 12–13 °C) alongside enriched $\delta^{18}O$ values, suggesting that the basin was not accumulating sediments at the onset of the WI as rising values in both proxies would be indicative of climatic amelioration between the Dimlington Stadial (DS) and the WI (e.g. Brooks and Birks, 2000; Brooks et al., 2012). The onset of sedimentation at Tirinie therefore appears later than at other sequences in Scotland (ca 14.6 cal ka BP; Matthews et al., 2011; Walker and Lowe, 2017) and the transition from Greenland Stadial 2.1 (GS-2.1) to Greenland Interstadial 1 (GI-1) in the NGRIP Greenland ice-core record (14.65 cal ka BP; Rasmussen et al., 2006, 2014). Delayed sediment accumulation may result from the presence of lingering or stagnant ice or snow-banks in upland locations following regional deglaciation in Scotland (e.g. Clark et al., 2012; Walker and Lowe, 2017).

Immediately following early-WI climatic warmth, between 14.1 ± 0.31 and 13.93 ± 0.12 cal ka BP, is a phase of oxygen isotopic depletion (TIR-O1; −2.32‰). Broadly contemporaneous with this shift to depleted $\delta^{18}O$ values (Section 6.2) summer temperatures decline from 11.3 ± 1.2 °C to 8.8 ± 1.1 °C (TIR-C_e1; 2.5 °C). The decline in summer temperatures relate to a shifting chironomid assemblage with greater abundances of the ultra-cold taxon *Micropsectra radialis*-type and cold climate taxa *Tanytarsus lugens*-type and *Micropsectra insignilobus*-type. Depletion in $\delta^{18}O$ and a reduction in C-ITs suggest a period of climatic deterioration at this time with the depression of both mean annual and mean July temperatures.

Within chronological uncertainty, this deterioration appears as a British correlative of Greenland Interstadial event 1d (GI-1d) dated from 14.07 to 13.90 cal ka BP (Rasmussen et al., 2014). Climatic deteriorations comparable to GI-1d have been identified towards the base of WI records across the British Isles, typically between the Borrobol and Penifiler Tephra horizons (Matthews

et al., 2011). Across Britain these deteriorations exhibit mean July temperature declines between 2 and 5.6 °C (Brooks and Birks, 2000; Marshall et al., 2002; Lang et al., 2010; Brooks et al., 2012, 2016).

From 13.93 ± 0.12 cal ka BP, the climate system recovers with an increase in C-ITs (*ca* 12 °C) driven by a loss of ultra-cold taxa and an initial increase in *Sergentia coracina*-type, followed by the cool temperate taxa *Tanytarsus glabrescens*-type, *Parakiefferiella*-type A and *Cricotopus laricomalis*-type. A return to enriched $\delta^{18}O$ values further suggests elevated mean annual temperatures throughout the mid-WI.

During the latter half of the WI at Tirinie, between 13.5 ± 0.28 and 13.06 ± 0.15 cal ka BP, a second cold climatic oscillation (Fig. 7) exhibits depletion in $\delta^{18}O$ (TIR-O2; −2.9‰) and a reduction in C-ITs from 11.9 ± 1.3 °C to 10.1 ± 1.1 °C (TIR-C_e2; 1.8 °C). Mean July temperature declines are driven by increased abundances of *Tanytarsus lugens*-type, *Sergentia coracina*-type and *Corynocera ambigua*. Isotopic depletion at this time appears greater than depletion associated with the earlier climatic deterioration (TIR-O1). However, owing to the lack of carbonate production in unit TIR-L3, the reconstructed isotopic values represent minimum isotopic depletion only and the true isotopic value of TIR-O1 may therefore be more depleted than TIR-O2 (Candy et al., 2016).

The late-WI climatic deterioration is coincident with the GI-1b climatic deterioration in Greenland, from 13.26 to 13.05 cal ka BP (Rasmussen et al., 2014). This climatic oscillation remains poorly identified and dated across the British Isles, but sites with sufficient proxy resolution record mean July temperature declines of 1.0–2.5 °C at similar stratigraphic positions (Brooks and Birks, 2000; Bedford et al., 2004; Brooks et al., 2012; van Asch et al., 2012).

A short period of climatic recovery during the late-WI at Tirinie is demonstrated by warm mean July temperatures (*ca* 13 °C). This short period of warming at the end of the WI is succeeded by climatic changes associated with the Loch Lomond Stadial (LLS) from 12.82 ± 0.29 cal ka BP (Fig. 7). Within age error this transition is comparable to the shift into the Younger Dryas across Europe (Muschitiello and Wohlfarth, 2015) and to GS-1 in Greenland (Rasmussen et al., 2014). Between 12.82 ± 0.29 and 11.71 ± 0.26 cal ka BP mean July temperatures fall from 11.7 ± 1.2 °C to 7.0 ± 1.2 °C which is driven by increases in the cold climate indicators *Corynocera ambigua* and *Tanytarsus lugens*-type. Unfortunately, negligible carbonate production throughout this phase precluded stable isotopic analyses. Alongside the decline in summer temperature, the identification of the Vedde Ash further confirms the LLS attribution of this phase (Candy et al., 2016). The coldest reconstructed temperatures throughout the sequence occur immediately following the deposition of the Vedde Ash. It is possible that the mechanisms for late LLS cooling at Loch Ashik, Isle of Skye (e.g. Brooks et al., 2012) can be invoked at Tirinie. At Loch Ashik, it has been suggested that enhanced winter precipitation (e.g. MacLeod et al., 2011) led to increased incidence of long-lasting snow beds. Spring and summer melting of these proximal snow beds decreased water temperatures and influenced C-IT reconstructions (Brooks et al., 2012). Being at a higher altitude than Loch Ashik the presence of long-lived snow beds during the LLS is likely and the disequilibria between water and air temperatures is possible. Alternatively, cold katabatic winds sourced from the West Highland Ice Field or more localised glacial centres including the Gaick plateau (e.g. Chandler et al., 2019) may have resulted in lower mean July temperatures.

A return to carbonate sedimentation (TIR-L8), elevated temperatures (*ca* 11–14 °C) and enriched $\delta^{18}O$ indicates climatic amelioration during the EH from 11.71 ± 0.26 cal ka BP. The timing of this transition is consistent with the onset of Holocene warming within Greenland (Rasmussen et al., 2007, 2014). Climatic warmth at Tirinie was punctuated by a final period of climatic deterioration between 11.5 ± 0.35 and 11.2 ± 0.42 cal ka BP. In contrast to the events from the WI, there is no evidence of C-IT variability during the EH with the sample resolution obtained. Therefore, $\delta^{18}O$ depletion (TIR-O3; −1.74‰) is the only direct measure of Holocene climatic instability at this location. Whilst it is acknowledged that the resolution of the C-IT record is not sufficient through this phase, chironomid samples were extracted from the most isotopically depleted area of the profile. Thus, greater confidence is gained from the suggestion of limited summer temperature decline but annual cooling over this phase of the EH at Tirinie.

Comparable early Holocene climatic deteriorations are difficult to disentangle with evidence of multiple episodes of climatic instability between 11.4 and 10.8 cal ka BP (Fiłoc et al., 2018). This includes an event in Greenland between 11.47 and 11.35 cal ka BP (Rasmussen et al., 2007, 2014) and the classically defined Pre-Boreal Oscillation (PBO) between 11.4 and 11.1 cal ka BP (e.g. Björck et al., 1997; Lang et al., 2010). Given the bounding chronology for the event at Tirinie it is reasonable to suggest that the climatic deterioration is comparable to the 11.4 ka event in Greenland, a phase of the PBO and minor mean July temperature declines identified at similar stratigraphic positions in Britain (Lang et al., 2010; Blockley et al., 2018).

5.5. Environmental and landscape responses to climatic change

The basal sediment from Tirinie (TIR-L1) is composed of silty clay. These sediments alongside a palynological profile consisting of open grassland taxa (TIR-P1; Poaceae, Cyperaceae, *Rumex*, and *Artemisia*) suggest relatively open, unstable landscapes until 14.11 ± 0.33 cal ka BP (Fig. 7). These pioneering taxa reflect the colonisation of exposed substrates, demonstrating a lag in vegetation development when compared with the warm climates of this interval (e.g. Walker and Lowe, 2017). Whilst *Betula* and *Pinus* are recorded, it is probable that *Pinus* reflects a far-travelled component (e.g. Birks et al., 2005) with *Betula* (likely *B. nana*) existing sporadically in the catchment. Throughout this initial phase low pollen concentrations (Supplementary Information 1), low Total Organic Carbon (TOC) and relatively enriched $\delta^{13}C$ values demonstrate low vegetation densities in the Tirinie catchment. The enriched $\delta^{13}C$ signal is likely reflective of lake waters, the dissolved inorganic carbon (DIC) pool, being composed of atmospheric CO_2 which exhibits higher $\delta^{13}C$ values compared to plant respired CO_2 (Talbot, 1990; Candy et al., 2016).

An increase in percentages of $CaCO_3$ (TIR-L2) suggest a reduction of clastic sedimentation through reduced allogenic sediment loading and increased catchment stabilisation. Greater abundances of *Empetrum nigrum* suggest the establishment of heathland (TIR-P1). The continued presence of open-habitat taxa further suggests incomplete heathland coverage with the formation of a grassland/heathland mosaic. The presence of *E. nigrum* alongside warm climates, indicates relatively high moisture availability during the early-WI at Tirinie (Bell and Tallis, 1973).

In response to the cold climatic deterioration between 14.1 ± 0.31 and 13.93 ± 0.12 cal ka BP, reductions of *Empetrum* and increases in Poaceae, Cyperaceae and disturbed ground indicators including *Rumex* and *Artemisia* (TIR-P2) suggest that heathland was replaced by open grassland. The shift in the Principal Curve (PrC) to more positive values signifies widespread compositional change (Simpson and Birks, 2012; Abrook et al., 2020). The loss of *Empetrum* from the landscape and increase in xerophytic taxa, including *Artemisia*, signifies a reduction in moisture availability during this climatic deterioration with a return to clastic sedimentation suggesting catchment erosion following landscape destabilisation. Increased charcoal, which coincides with a reduction in TLP

concentration (TIR-P2; Supplementary Information 1), following this change in vegetation structure indicates that fire was an important response variable to climatic and environmental change (TIR-Ch1; Figs. 3 and 7).

Climatic improvement during the mid-WI initially favoured the re-establishment of heathland and precipitation of lacustrine marl. Subsequently, increases in *Juniperus* (TIR-P3) indicates the development of a *Juniperus* scrub, perhaps reflecting greater soil maturation (Preston et al., 2002). *Juniperus* establishment (13.68 ± 0.27 cal ka BP; TIR-P3a) may also confirm *Betula* being dwarf shrub *B. nana*. However, an increase in *Betula* pollen (TIR-P3b) may suggest a greater colonisation of dwarf birch with the addition of sparse and localised tree birch. Warm summer temperatures during the mid-WI (Section 5.4) and enhanced soil maturity reveal suitable conditions for tree birch establishment (Birks, 1994). Evidence for tree birch during middle of the WI in Scotland is supported from the identification of a tree birch fruit from Abernethy Forest (Birks and Mathewes, 1978) *ca* 50 km north of Tirinie. *Betula* spp. development may also explain depletion in $\delta^{13}C$ with greater plant respired CO_2 being delivered to vadose and lake waters (Candy et al., 2016).

The climatic deterioration between 13.5 ± 0.28 and 13.06 ± 0.15 cal ka BP drives a second shift in landscape and environment. A reduction in *Betula* with increased herbaceous pollen suggests a contraction of woody taxa and expansion of open herbaceous vegetation (TIR-P4). The open ground assemblage is dominated by disturbance indicators including Poaceae and *Rumex* but also Caryophyllaceae, Asteraceae, and Lactuceae. Whilst reduced percentages of woody pollen could indicate a reduction in flowering ability under a period of climatic stress, the Arctic/alpine community identified here is more indicative of landscape replacement under a background of climatic change. If a reduction in flowering ability were to occur, this might be instantaneous, however, *Betula* concentrations rise (Supplementary Information 1) following isotopic depletion, which occurs prior to the shift in lithostratigraphy. This lithostratigraphic shift results in increased TOC which is thought to reflect allogenic loading in the basin following the in-washing of mid-WI soils. Subsequently, increased macro-charcoal (TIR-Ch2) indicates greater fire activity in the Tirinie catchment. This occurs following reduced concentrations of pollen from woody vegetation and an increase in concentrations from open ground taxa (TIR-P4; Supplementary Information 1) suggesting that charcoal abundance is not driven by changes in sedimentation rate and therefore reflects fire dynamics.

A return to favourable climatic conditions during the late-WI occurs alongside a resumption of marl sedimentation and a return to a juniper scrub dominated landscape (TIR-P5). However, the climatic deterioration associated with the LLS between 12.82 ± 0.29 and 11.71 ± 0.26 cal ka BP caused whole-scale environmental changes (Fig. 7). Coeval with the reduction in temperature, woody vegetation in the catchment contracted, increasing landscape instability and allogenic sediment loading, likely through enhanced periglacial activity (e.g. Pennington et al., 1972; Walker, 1975; Walker and Lowe, 1990, 2017). The vegetation assemblage of this interval (TIR-P5; TIR-P6) was characterised by an open grassland, with *Artemisia*, *Rumex* and Poaceae, occurring alongside Caryophyllaceae, Lactuceae, Saxifragaceae, *Thalictrum* and the pteridophyte *Selaginella selaginoides*. Many of these taxa occur in present day steppic/tundra environments and on soils prone to solifluction or cryoturbation (Birks and Mathewes, 1978; Brysting et al., 1996; Mayle et al., 1997). The continued presence of *Salix* and *Empetrum* may indicate greater protection from cold climatic conditions, either in sheltered localities or within seasonal snow beds. Late LLS increases in *Artemisia*, after *ca* 12.0 cal ka BP, coincide with the coldest temperatures of the LLS; which also may demonstrate that the latter half of the LLS was particularly dry at this location. This is a possibility at Tirinie, in the lee of the LLS West Highland Ice Field (e.g. Lowe et al., 2019; Palmer et al., 2020), with ice accumulation scavenging moisture creating more arid conditions to the east. The increase in *Pediastrum* throughout the LLS adds credence to this suggestion as it is possible that with limited precipitation, reduced lake levels allowed *Pediastrum* to bloom in the shallow lacustrine system.

Climatic reorganisation and warmth during the EH from 11.71 ± 0.26 cal ka BP led to the renewed precipitation of $CaCO_3$ in the Tirinie basin and the contraction of LLS Arctic/alpine vegetation. The continued presence of Poaceae and Cyperaceae suggests that during the earliest Holocene an open grassland community persisted in the catchment (TIR-P7). The expansion of the oligotrophic *Myriophyllum* (Edwards and Whittington, 2010) and reduction in *Pediastrum* coenobia demonstrates a return to higher lake levels at this time.

The remainder of the EH displays a typical successional sequence observable across much of Scotland (e.g. Mayle et al., 1997; Kelly et al., 2017) with the establishment of successive phases of *Empetrum* heathland (TIR-P8), *Juniperus* scrub (TIR-P9), *Betula* woodland (TIR-P11) with *Corylus* becoming established by 10.01 ± 0.60 cal ka BP. However, palynological variability between 11.48 ± 0.35 and 11.17 ± 0.43 cal ka BP (TIR-P8) is attributed to fluctuations in *Betula* and *Empetrum* with small increases in Poaceae and *Rumex*, and a spike in spores of *Equisetum*. Through this phase a heathland/grassland mosaic existed in the Tirinie catchment. Following a period of enhanced annual climatic variability, it is postulated that a contraction of the water body lowered lake levels allowing the proliferation of *Equisetum*. The plateau in the PrC, as opposed to a reversal, reveals that vegetation changes in the EH were more subdued that the WI. As with other vegetation responses to abrupt climatic change, fire appears to be an important component of the landscape but only following shifts in the vegetative structure of the environment.

6. Discussion

6.1. Comparison of climatic and palynological variability across Europe

Few studies perform reconstructions using similar proxies at similar temporal resolutions as this study. However, a select number of sequences, Fiddaun, Gerzensee, and Hässeldala Port (Table 5) do, permitting a comparison of variability across Europe.

Climatic and environmental variability across these key sites show comparability in timing. These events all show, with the exception of the C-ITs at Gerzensee, depletion in $\delta^{18}O$ and reductions in mean July temperature. As a minimum each site exhibits both the GI-1d (Aegelsee oscillation) and the GI-1b (Gerzensee oscillation) equivalent event, whilst only those that extend to the Holocene exhibit the 11.4 ka event. It is clear that discrepancies exist in the magnitude of proxy variability across Europe (Table 5) both between sites and events. This likely relates to differences in the magnitude of climatic change across Europe and the influence of continentality, altitude and the distance from an oceanic heat source (e.g. Leng and Marshall, 2004). However, this discussion is beyond the scope of this paper.

Unsurprisingly, landscape responses to these events are variable (Table 5). This is in part a product of the location of sites across Europe and variable rates of plant migration, but also the amplitude of climatic change. All sites exhibit an increase or the continued presence of open ground herbaceous communities for the GI-1d-equivalent event, which in central Europe relates to the opening of birch forests (Ammann et al., 2013) compared to contractions in

Table 5
Comparative studies from Europe using the same proxies as the present study. Given are changes associated with each event across each proxy and their approximate age. NGRIP is also shown here. *Temperature increases as taxon change suggested to be driven by additional factors other than temperature (Lotter et al., 2012).

Site	Approximate Age (cal ka BP)	Oxygen Isotopes	C-IT	Vegetation	Reference
Tirinie	14.0	−2.32‰	−2.5 °C	↑ Open ground assemblages	This study
	13.2	−2.9‰	−1.8 °C	↑ Open ground assemblages	
	11.4	−1.74‰	n/a	↑ *Equisetum*, Poaceae	
Fiddaun	14.0	−1‰	−1.0 °C	↑ Herbaceous communities	van Asch et al. (2012); van Asch and Hoek (2012)
	13.1	−1‰	−1.5 °C	↓ *Betula* ↑ Poaceae	
Gerzensee	14.0	−1‰	+1.5 °C *	↑ Open ground assemblages	Schwander et al. (2000); Lotter et al. (2012); Ammann et al. (2013); van Raden et al. (2013)
	13.1	−1.1‰	−0.5 - 1°C	*Pinus* dominant	
	11.2	−1.0‰	n/a	↓ *Pinus* ↑ *Betula*	
Hässeldala Port	14.0	n/a	−0.5 - 1 °C	Open ground communities	Wohlfarth et al. (2006); Watson (2008); Wohlfarth et al. (2017)
	13.1	n/a	−2.0 °C	↓ *Betula* ↑ *Pinus*, *Empetrum*	
Greenland	14.0 (GI-1d)	−2.9‰	n/a	n/a	Rasmussen et al. (2007); Rasmussen et al. (2014)
	13.2 (GI-1b)	−2.5‰	n/a	n/a	
	11.45 (11.4)	−1.82‰	n/a	n/a	

shrub/heath vegetation in the west (van Asch and Hoek, 2012). In central Europe, for the GI-1b-type event, pine forests are dominant (Ammann et al., 2013) with limited expansion of herbaceous vegetation. Contrastingly, over the same period, the floral community in west and coastal north Europe was not as developed, permitting the expansion of open ground indictors (this study; van Asch and Hoek, 2012) and *Empetrum* and *Pinus* (Wohlfarth et al., 2017). Therefore, clear disparities exist across Europe in the expression of abrupt events.

6.2. Asynchrony of climatic drivers and vegetation responses

Whilst disparities between sites are known, an understanding of phase relationships (outside of regions than contain annually laminated archives) remain largely unknown as many studies reconstruct only single climatic or environmental parameters or correlate multiple parameters using different sedimentary sequences or sites. This correlation approach is problematic as it may introduce matching errors which obscure patterns of climatic and environmental change. However, where reconstructions are performed on single sequences (e.g. van Asch et al., 2012; Ammann et al., 2013; Whittington et al., 2015) inferences into the relationships between proxies can be gained alongside an understanding of the mechanisms of change. This discussion centres on the stratigraphic phasing of changes at Tirinie placed on the indicative chronology (Fig. 8). This approach is valid as the onset of proxy variability can be measured precisely, i.e. with depth, and will not change. Differences in stratigraphic placement must therefore relate to differences in timing with measurable differences in lag. We acknowledge that this analysis is sensitive to proxy sampling intervals, however, over each event sampling is either contiguous or near contiguous for each proxy (Section 3).

6.2.1. Event 1

For the ca 14.0 ka event at Tirinie, the onset of isotopic depletion occurs at 352 cm (14.1 cal ka BP) whilst the onset of mean July temperature change occurs at 351 cm (14.06 cal ka BP) indicating multi-decadal lags of ~40 years. It is noted that the onset of this event follows a general trend of decreasing July temperatures. However, this trend of declining temperatures is within sample specific errors. Therefore, the point at which C-IT variability falls outside of the error of the technique is taken as the onset of mean July temperature change. It is only following oxygen isotopic depletion and C-IT declines that palynological responses occur (Fig. 8). Furthermore, at the point of palynological variability, a shift to clastic sedimentation occurs. These changes are subsequently followed by increases in charcoal.

6.2.2. Event 2

For the ca 13.2 ka event greater asynchrony is observed in the phasing of climatic and environmental parameters. Isotopic depletion occurs from 340.5 cm (13.5 cal ka BP) which is followed by mean July temperature declines from 337 cm (13.28 cal ka BP) suggesting a centennial lag of ~200 years. The palynological response occurs from 339 cm (13.4 cal ka BP) ~100 years after isotopic depletion, with a strengthening of palynological change from 337 cm (13.28 cal ka BP) ~100 years later. Much like Event 1 the shift to clastic sediments and increased charcoal production occurs following the palynological shift. However, Event 2 exhibits additional complexity and structure not only with a two-stage palynological response but also with peaks in charcoal across both phases of palynological/clastic variability.

6.2.3. Event 3

During the early Holocene climatic variability is only recorded in oxygen isotopic data suggesting limited summer temperature change. $\delta^{18}O$ depletions occur at 281 cm (11.5 cal ka BP) with the palynological response occurring from 280 cm (11.48 cal ka BP) suggesting a decadal lag. Minor lithostratigraphic changes are noted in association with the isotopic depletion and greater charcoal frequencies are present throughout the event (Fig. 8).

We suggest that the offset between isotopic depletion and July temperature change can be explained through oceanic mechanisms invoked for climatic deteriorations. Principally through the weakening of Atlantic Meridional Overturning Circulation (AMOC) following the release of freshwater into the North Atlantic (e.g. Clark et al., 2001; Tarasov and Peltier, 2005; Thornalley et al., 2010). The effect of enhanced cold water and/or reduced salinity gradients in the North Atlantic subpolar gyre results in greater stratification between surface and bottom waters (e.g. Broecker et al., 1989; de Vernal et al., 1996; Tarasov and Peltier, 2005; Haskins et al., 2019). In turn, North Atlantic Bottom Water (NADW) formation is supressed and AMOC is weakened (Condron and Winsor, 2012; Haskins et al., 2019), leading to a reduction of heat transport to the northern high latitudes (Clark et al., 2001). Modelled evidence suggests that perturbations to AMOC are coincident with seasonal sea ice extending towards the lower latitudes (e.g. Isarin et al.,

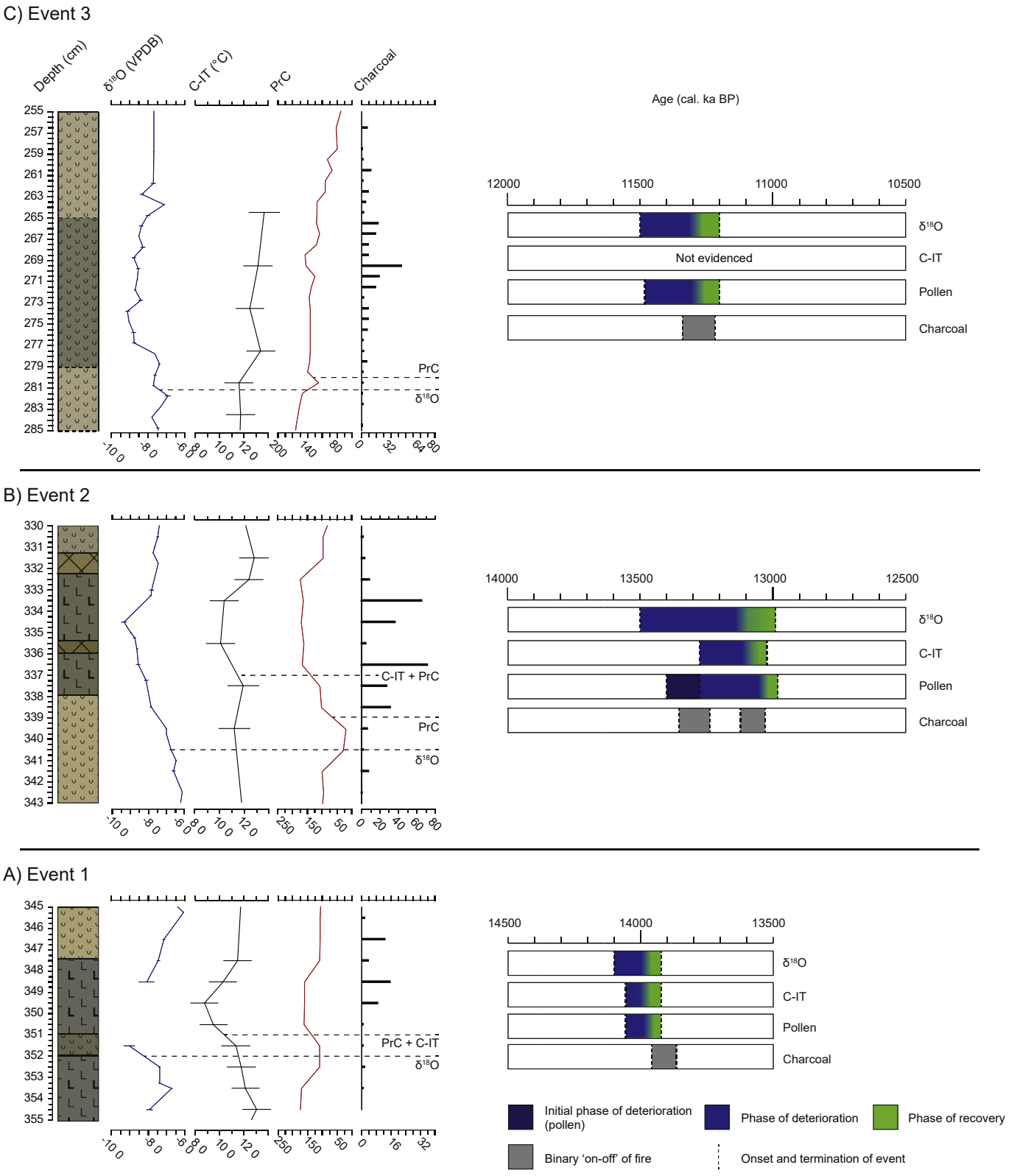

Fig. 8. The anatomy of climatic events from the Tirinie profile. Panels on the left show the data from the Tirinie sequence with panels on the right showing a schematic of change. A) Highlighting the asynchrony of climatic and environmental parameters for Event 1 (GI-1d-type); B) Event 2 (GI-1b-type); and C) Event 3 (11.4 ka-type). Within each schematic in the right panel the position and age of the gradient fill is directly related to the position of the dashed lines in the left panel. In selecting thresholds, we have taken a point between samples where changes occur that are outside the error of the technique and/or sustained for multiple samples. (For interpretation of the references to colour in this figure legend, the reader is referred to the Web version of this article.)

1998; Isarin and Renssen, 1999; Bakke et al., 2009). This seasonal sea ice expansion would induce the southward migration of the polar jet leading to heightened seasonal variations in thermal conditions. Therefore, the offset between isotopic and C-IT variability is thought to reflect winter temperature change (see Section 5.3) through the migration of the polar jet. Heightened seasonality would be further exacerbated with positive feedbacks in sea ice production through increased albedo. At a critical point in this model it is postulated that either AMOC further weakens or sea ice extension is no longer restricted to the winter season, resulting in a greater temporal depression of the polar jet and summer temperature declines. Therefore, whilst there is an offset between winter and summer temperature change for most events, at a critical point different modes of temperature variability converge.

Palynological responses (Fig. 8) to these abrupt climatic changes appear strongest following the initiation of both winter and subsequent mean July temperature declines (e.g. Event 1) suggesting the passing of plant physiological thresholds. *Betula* tree species have an 11 °C to 12 °C lower summer temperature limit (van Dinter and Birks, 1996; Birks and Birks, 2014) whilst *Betula nana* has a 6 °C summer temperature limit (de Groot et al., 1997). Additional woody species that decline during these events are *Empetrum* and *Juniperus* although both are tolerant of cold climatic conditions (Thomas et al., 2007). The strongest palynological shifts associated with climatic deteriorations at Tirinie, occurs when July temperatures fall below 11 °C. As *Empetrum* and *Juniperus* favour well-drained soils (Thomas et al., 2007; Birks and Birks, 2014), it is postulated that their contraction is a result of the climatically-mediated change in soil moisture conditions. Following the contraction of woody taxa there is a period of reduced landscape stability and clastic sedimentation, where continued cold annual and summer climates combined with less stabilising open herbaceous vegetation (*Artemisia*, *Rumex* and Poaceae respectively) likely led to the enhancement of erosive and transportative capacity from the surrounding slopes and river networks feeding into Tirinie.

The model above fits with existing theories of how landscapes might respond to climatic transitions (e.g. van Asch and Hoek, 2012). However, the data presented here suggests this model is too simplistic. This is clearly seen in the two-stage response for Event 2 (Fig. 8). At the onset of this event *Betula* expands despite the reduction in mean annual (winter) temperatures. From 13.4 cal ka BP variability in the PrC, driven by changes in *Betula*, reflect the contraction of *Betula* in the landscape. Contractions of *Betula* therefore appear to coincide with a prolonged period of reduced mean annual (winter) temperatures. However, as *Betula* is not limited by winter temperatures (tree birch can tolerate winter temperatures of −20 °C to −30 °C; Birks and Birks, 2014) it is not clear what drives these changes. It is postulated that these shifts reflect the effects of enhanced temperature gradients across the year and increased seasonal sea ice in the North Atlantic on aridity/moisture availability. In this model it is probable that aridity would result with the deflection of storm tracks following the expansion of sea ice. However, quantifiable aridity indicators are required to test this. A secondary shift in the PrC is driven by a further contraction in *Betula* following enhanced annual and summer temperature declines. Non temperature factors (e.g. aridity/fire) or the effect of low annual temperatures on the growing season are therefore clearly important in understanding widespread catchment destabilisation in association with Event 2.

In the Holocene (Event 3) the annual temperature signal has no apparent summer temperature component. Therefore, the same process is not observed. Here, it is proposed that winter temperature shifts alongside aridity caused a contraction of lake waters allowing for an expansion of *Equisetum*. Whilst the structure of the event is different, it is likely that aridity is an important factor.

6.3. Event recovery

Climatic and environmental recovery following each event is clearly shown within the Tirinie stratigraphy. Principally oxygen isotopic enrichment and C-IT increases reveal climatic amelioration, which in the model suggested above may be a product of AMOC strengthening and the northward retreat of sea ice and the polar jet. Climatic amelioration then provides a mechanism for the re-establishment of woody vegetation. The vegetational recovery associated with Event 1 and Event 3 exhibit a return to similar vegetation evidenced prior to the climatic oscillation (*Empetrum* and dwarf *Betula*). Being earlier in the successional sequence, vegetation which can survive on skeletal or impoverished soils would rapidly recolonise the landscape. However, the recovery in vegetation following Event 2 is dissimilar to preceding vegetation types (dwarf and tree *Betula*). The establishment of a *Juniperus* scrub alongside climatic improvement relate to unsuitable environmental conditions for *Betula* colonisation despite temperatures being suitably warm (e.g. van Dinter and Birks, 1996). This difference therefore perhaps relates to a lag in *Betula* migration following its removal or a lack of moisture availability immediately following the event (Birks and Birks, 2014). Following each of these events, recovery of vegetation leads to landscape stabilisation and the resumption of carbonate sedimentation. Therefore, carbonate deposition marks the termination of each climatic event.

6.4. The role of fire in the LGIT

In Britain there is considerable palaeofire research associated with Holocene (e.g. Moore, 2000; Innes et al., 2010; Grant et al., 2014; Edwards et al., 2019), although this is often overlooked in many LGIT studies. This is perhaps due to both the development of widespread woodland during the Holocene and the continuous human occupation of Britain from the Mesolithic; both features that enhance fire frequency. Thus, the role of fire as an agent of landscape change during the earlier phases of the LGIT has not been fully explored (Edwards et al., 2000). At Tirinie whilst there is a background signal of charcoal throughout the profile, greater fire activity appears to be associated with climatic events.

Fire activity occurs after the onset of mean annual (winter) and summer temperature declines and following a shift in vegetation for all events (Event 1; 2; 3). These features have previously been identified but are associated with warming and drying climates/enhanced biomass on the landscape (Marlon et al., 2009; Grant et al., 2014). However, these findings are often realised in the absence of local climatic data (Walker et al., 2012) or associated with shifts in vegetation assemblage which are not necessarily congruent with climatic shifts (e.g. Edwards et al., 2007; and caveats therein). In this study, fire is an important landscape component within each defined climatic event prior to recovery (Fig. 8). However, the fire-landscape relationship is more complex when considering individual events.

The greatest incidence of fire occurs within the two-stage response for Event 2. This is not surprising considering the abundance of woody vegetation (*Betula*) on the landscape. However, *Betula* has previously been suggested to exhibit a negative feedback with fire (e.g. Jeffers et al., 2012) perhaps due to its low combustibility (Carcaillet et al., 2001). Whilst reductions in *Betula* occur marginally prior to enhanced wildfire, the two factors occur together, precede summer temperature variabilty and occur alongside annual (winter) temperature change. These features suggest that alongside aridity (Section 6.3), fire may have assisted the opening of the landscape at this time. This first stage of Event 2 notwithstanding, with available data it is probable that for each event, alongside climatic deteriorations, an increase in fuel

availability (woody vegetation) led to increased burning.

In a model where fire is a response to climatic deterioration and either follows or is associated with vegetation change, in the absence of human influence, the incidence of fire is likely a direct result of changing atmospheric configurations or changing pressure gradients which accompany these climatic events (e.g. Isarin and Renssen, 1999; Brauer et al., 2008). Therefore, a clear connection between atmosphere and environment exists at Tirinie, which is mediated by feedbacks with the dominant vegetation types (*Empetrum*, *Betula*) and fire (Jeffers et al., 2012).

7. Conclusions

The presented multi-proxy investigation from Tirinie provides a highly resolved and chronologically constrained record of climatic and environmental variability from the LGIT within the Grampian Highlands in Scotland. We identify millennial-scale climatic and environmental changes as seen across the North Atlantic region. However, we also identify a series of centennial-scale climatic events (Event 1; 2; 3), which exhibit environmental/landscape responses, that are British correlatives of the GI-1d, GI-1b and 11.4 ka events in Greenland. Further, we show that across key sites the timing of comparable events is similar, but the expression of the events differ. Importantly, our approach reveals phase differences between different climatic (mean annual and summer temperature) and environmental (vegetation, fire, lithological expression) parameters, which are dissimilar for each event. We suggest that phase differences can be explained by the of mode of climatic change, linked to AMOC variability and the seasonal expansion of sea ice. However, additional complexities, including a two-stage response for Event 2, including multiple fire episodes; and a single response for Event 3, without summer temperature change, can be observed. Additionally, therefore, we suggest that aridity/moisture availability is a crucial unknown climate component and control on environments in north-west Europe during the LGIT.

These differences and complexities need to be tested across wider range of locations as this is an individual site recording three events. If the inferences made here are shown to be robust then lags between climatic change and environmental response varies between the phasing of mean annual and summer temperature changes. This observation suggests that the validity of using palynology alone as a tool to match climate records should be questioned when used at centennial-scales and highlights the value of the combination of proxy sources used in this study.

Declaration of competing interest

The authors declare that they have no known competing financial interests or personal relationships that could have appeared to influence the work reported in this paper.

Acknowledgements

The authors would like to thank two anonymous reviewers for helpful and constructive reviews and recommendations which have significantly improved the quality of this manuscript. The authors would further like to thank Professor John Lowe, Professor Michael Walker, Dr Dirk Sachse and David Maas for constructive discussions regarding the data presented within this manuscript. C.F would like to acknowledge Dr Stefan Engels for discussions and assistance in the statistical treatment of chironomid data and Professor Oliver Heiri and colleagues for making the combined Swiss-Norwegian dataset available online. The authors would also like to express many thanks to MSc students at Royal Holloway for assistance in collecting sedimentary material from the Tirinie site and Dr Marta Perez-Fernandez for technical and laboratory support.

Appendix A. Supplementary data

Supplementary data to this article can be found online at https://doi.org/10.1016/j.quascirev.2020.106634.

Author contributions

Ashley Abrook: Conceptualization; Resources; Methodology; Investigation; Formal analysis; Visualisation; Writing - original draft; Writing - review & editing, Ian Matthews: Conceptualization; Resources; Validation; Supervision; Writing - review & editing, Ian Candy: Investigation; Supervision; Writing - review & editing, Adrian Palmer: Supervision; Resources; Writing - review & editing, Chris Francis: Investigation; Formal analysis; Writing - review & editing, Lucy Turner: Investigation. Stephen Brooks: Validation; Supervision; Writing - review & editing. Angela Self: Investigation. Alice Milner: Conceptualization; Validation; Supervision; Writing - review & editing

Funding

This work was supported by the Natural Environmental Research Council [AA: Grant number NE/L002485/1] to facilitate palynological, statistical and isotopic analyses. Additional chironomid and statistical analyses was also supported by the Natural Environmental Research Council [CF: Grant number NE/L002485/1].

References

Abrook, A.M., Matthews, I.P., Milner, A.M., Candy, I., Palmer, A.P., Timms, R.G.O., 2020. Environmental variability in response to abrupt climate change during the Last Glacial-Interglacial Transition (16-8 cal ka BP): evidence from Mainland, Orkney. Scot. J. Geol. 56, 30–46.

Ammann, B., van Leeuwen, J.F., van der Knaap, W.O., Lischke, H., Heiri, O., Tinner, W., 2013. Vegetation responses to rapid warming and to minor climatic fluctuations during the Late-Glacial Interstadial (GI-1) at Gerzensee (Switzerland). Palaeogeogr. Palaeoclimatol. Palaeoecol. 391, 40–59.

Bakke, J., Lie, Ø., Heegaard, E., Dokken, T., Haug, G.H., Birks, H.H., Dulski, P., Nilsen, T., 2009. Rapid oceanic and atmospheric changes during the Younger Dryas cold period. Nat. Geosci. 2 (3), 202–205.

Bedford, A., Jones, R.T., Lang, B., Brooks, S., Marshall, J.D., 2004. 'A Late-glacial chironomid record from Hawes Water, northwest England. J. Quat. Sci. 19 (3), 281–290.

Bell, J.N.B., Tallis, J.H., 1973. Biological flora of the British Isles. *Empetrum nigrum* L.' *Journal of Ecology* 61 (1), 289–305.

Birks, H.J.B., Line, J.M., Juggins, S., Steveson, A.C., ter Braak, C.J.F., 1990. Diatoms and pH reconstruction, 327.' *Philosophical Transactions of the Royal Society of London B*, pp. 263–278.

Birks, H.H., 1994. Late-glacial vegetational ecotones and climatic patterns in Western Norway. Veg. Hist. Archaeobotany 3 (2), 107–119.

Birks, H.J.B., 1998. Numerical tools in palaeolimnology- progress, potentialities, and problems. J. Paleolimnol. 20, 307–332.

Birks, H.H., Birks, H.J.B., 2014. To what extent did changes in July temperature influence Lateglacial vegetation patterns in NW Europe? Quat. Sci. Rev. 106, 262–277.

Birks, H.H., Mathewes, R.W., 1978. Studies in the vegetational history of Scotland. V late devensian and early flandrian pollen and macro-fossil stratigraphy at Abernethy forest, inverness-shire. New Phytol. 80 (2), 455–484.

Birks, H.H., Larsen, E., Birks, H.J.B., 2005. 'Did tree-*Betula, Pinus* and *Picea* survive the last glaciation along the west coast of Norway? A review of the evidence, in light of Kullman (2002). J. Biogeogr. 32 (8), 1461–1471.

Björck, S., Rundgren, M., Ingolfsson, O., Funder, S., 1997. The Preboreal oscillation around the Nordic Seas: terrestrial and lacustrine responses. J. Quat. Sci. 12 (6), 455–465.

Björck, S., Walker, M.J.C., Cwynar, L.C., Johnsen, S., Knudsen, K.L., Lowe, J.J., Wohlfarth, B., 1998. 'An event stratigraphy for the Last Termination in the North Atlantic region based on the Greenland ice-core record: a proposal by the INTIMATE group. J. Quat. Sci. 13 (4), 283–292.

Blockley, S., Candy, I., Matthews, I., Langdon, P., Langdon, C., Palmer, A., Lincoln, P., Abrook, A., Taylor, B., Conneller, C., Bayliss, A., MacLeod, A., Deeprose, L., Darvill, C., Kearney, R., Beavan, N., Staff, R., Bamforth, M., Taylor, M., Milner, N.,

2018. The resilience of postglacial hunter-gatherers to abrupt climate change. Nature Ecology & Evolution 2 (5), 810–818.
Brauer, A., Haug, G.H., Dulski, P., Sigman, D.M., Negendank, J.F., 2008. An abrupt wind shift in western Europe at the onset of the Younger Dryas cold period. Nat. Geosci. 1 (8), 520–523.
Broecker, W.S., Kennett, J.P., Flower, B.P., Teller, J.T., Trumbore, S., Bonani, G., Wolfli, W., 1989. Routing of meltwater from the laurentide ice sheet during the younger Dryas cold episode. Nature 341 (6240), 318–321.
Bronk Ramsey, C., 2008. Deposition models for chronological records. Quat. Sci. Rev. 27 (1–2), 42–60.
Bronk Ramsey, C., 2009. Bayesian analysis of radiocarbon dates. Radiocarbon 51 (1), 337–360.
Bronk Ramsey, C., Albert, P.G., Blockley, S.P.E., Hardiman, M., Housley, R.A., Lane, C.S., Lee, S., Matthews, I.P., Smith, V.C., Lowe, J.J., 2015. Improved age estimates for key Late Quaternary European tephra horizons in the RESET lattice. Quat. Sci. Rev. 118, 18–32.
Brooks, S.J., Davies, K.L., Mather, K.A., Matthews, I.P., Lowe, J.J., 2016. 'Chironomid-inferred summer temperatures for the last glacial–interglacial transition from a lake sediment sequence in muir Park reservoir, west-central Scotland. J. Quat. Sci. 31 (3), 214–224.
Brooks, S.J., Langdon, P.G., Heiri, O., 2007. *The Identification and Use of Palaearctic Chironomidae Larvae in Palaeoecology*. QRA Technical Guide No. 10. Quaternary Research Association, London, p. 276pp.
Brooks, S.J., Matthews, I.P., Birks, H.H., Birks, H.J.B., 2012. High resolution Late-Glacial and early Holocene summer air temperature records from Scotland inferred from chironomid assemblages. Quat. Sci. Rev. 41, 67–82.
Brooks, S.J., Birks, H.J.B., 2000. 'Chironomid-inferred Late-glacial air temperatures at Whitrig Bog, southeast Scotland. J. Quat. Sci. 15 (8), 759–764.
Brooks, S.J., Birks, H.J.B., 2001. Chironomid-inferred air temperatures from Late-glacial and Holocene sites in north-west Europe: progress and problems. Quat. Sci. Rev. 20 (16), 1723–1741.
Brooks, S.J., Langdon, P.G., 2014. 'Summer temperature gradients in northwest Europe during the Lateglacial to early Holocene transition (15–8 ka BP) inferred from chironomid assemblages. Quat. Int. 341, 80–90.
Brysting, A.K., Gabrielsen, T.M., Sørlibråten, O., Ytrehorn, O., Brochmann, C., 1996. The Purple Saxifrage, Saxifraga oppositifolia, in Svalbard: two taxa or one? Polar Res. 15 (2), 93–105.
Candy, I., Abrook, A., Elliot, F., Lincoln, P., Matthews, I.P., Palmer, A., 2016. 'Oxygen isotopic evidence for high-magnitude, abrupt climatic events during the Late-glacial Interstadial in north-west Europe: analysis of a lacustrine sequence from the site of Tirinie, Scottish Highlands. J. Quat. Sci. 31 (6), 607–621.
Carcaillet, C., Bergeron, Y., Richard, P.J., Fréchette, B., Gauthier, S., Prairie, Y.T., 2001. Change of fire frequency in the eastern Canadian boreal forests during the Holocene: does vegetation composition or climate trigger the fire regime? J. Ecol. 89 (6), 930–946.
Carcaillet, C., Perroux, A.S., Genries, A., Perrette, Y., 2007. Sedimentary charcoal pattern in a karstic underground lake, Vercors massif, French Alps: implications for palaeo-fire history. Holocene 17 (6), 845–850.
Chandler, B.M.P., Boston, C.M., Lukas, S., 2019. A spatially-restricted Younger Dryas plateau icefield in the Gaick, Scotland: reconstruction and palaeoclimatic implications. Quat. Sci. Rev. 211, 107–135.
Clark, C.D., Hughes, A.L., Greenwood, S.L., Jordan, C., Sejrup, H.P., 2012. Pattern and timing of retreat of the last British-Irish Ice Sheet. Quat. Sci. Rev. 44, 112–146.
Clark, P.U., Marshall, S.J., Clarke, G.K., Hostetler, S.W., Licciardi, J.M., Teller, J.T., 2001. Freshwater forcing of abrupt climate change during the last glaciation. Science 293 (5528), 283–287.
Condron, A., Winsor, P., 2012. Meltwater routing and the younger Dryas. Proc. Natl. Acad. Sci. Unit. States Am. 109 (49), 19928–19933.
de Groot, W.J., Thomas, P.A., Wein, R.W., 1997. Biological flora of the British Isles: *Betula nana* L. And *Betula glandulosa* michx. J. Ecol. 85 (2), 241–264.
de Vernal, A., Hillaire-Marcel, C., Bilodeau, G., 1996. Reduced meltwater outflow from the Laurentide ice margin during the Younger Dryas. Nature 381 (6585), 774–777.
Edwards, K.J., Whittington, G., 2010. Lateglacial palaeoenvironmental investigations at Wester Cartmore Farm, Fife and their significance for patterns of vegetation and climate change in east-central Scotland. Rev. Palaeobot. Palynol. 159 (1–2), 14–34.
Edwards, K.J., Bennett, K.D., Davies, A.L., 2019. Palaeoecological perspectives on Holocene environmental change in Scotland. Earth and Environmental Science Transactions of the Royal Society of Edinburgh 110 (1–2), 199–217.
Edwards, K.J., Langdon, P.G., Sugden, H., 2007. Separating climatic and possible human impacts in the early Holocene: biotic response around the time of the 8200 cal yr BP event. J. Quat. Sci. 22 (1), 77–84.
Edwards, K.J., Whittington, G., Tipping, R., 2000. The incidence of microscopic charcoal in late glacial deposits. Palaeogeogr. Palaeoclimatol. Palaeoecol. 164 (1–4), 247–262.
Fægri, K., Iversen, J., 1989. Textbook of Pollen Analysis, fourth ed. John Wiley and Sons, Chichester, p. 340pp.
Fiłoc, M., Kupryjanowicz, M., Rzodkiewicz, M., Suchora, M., 2018. Response of terrestrial and lake environments in NE Poland to Preboreal cold oscillations (PBO). Quat. Int. 101–117.
Grant, M.J., Hughes, P.D., Barber, K.E., 2014. 'Climatic influence upon early to mid-Holocene fire regimes within temperate woodlands: a multi-proxy reconstruction from the New Forest, southern England. J. Quat. Sci. 29 (2), 175–188.
Grimm, E.C., 1987. CONISS: a FORTRAN 77 program for stratigraphically constrained cluster analysis by the method of incremental sum of squares. Comput. Geosci. 13 (1), 13–35.
Haskins, R.K., Oliver, K.I., Jackson, L.C., Wood, R.A., Drijfhout, S.S., 2019. Temperature domination of AMOC weakening due to freshwater hosing in two GCMs. Clim. Dynam. 1–14.
Heiri, O., Lotter, A.F., 2001. Effect of low count sums on quantitative environmental reconstructions: an example using subfossil chironomids. J. Paleolimnol. 26, 343–350.
Heiri, O., Lotter, A.F., Hausmann, S., Kienast, F., 2003. A chironomid- based Holocene summer air temperature reconstruction from the Swiss Alps. Holocene 13, 477–484.
Heiri, O., Cremer, H., Engels, S., Hoek, W.Z., Peeters, W., Lotter, A.F., 2007. Lateglacial summer temperatures in the Northwest European lowlands: a chironomid record from Hijkermeer, The Netherlands. Quat. Sci. Rev. 26 (19), 2420–2437.
Innes, J., Blackford, J., Simmons, I., 2010. Woodland disturbance and possible land-use regimes during the Late Mesolithic in the English uplands: pollen, charcoal and non-pollen palynomorph evidence from Bluewath Beck, North York Moors, UK. Veg. Hist. Archaeobotany 19 (5–6), 439–452.
Isarin, R.F., Renssen, H., 1999. Reconstructing and modelling late weichselian climates: the younger Dryas in Europe as a case study. Earth Sci. Rev. 48 (1–2), 1–38.
Isarin, R.F., Renssen, H., Vandenberghe, J., 1998. The impact of the north atlantic ocean on the younger Dryas climate in northwestern and central Europe. J. Quat. Sci. 13 (5), 447–453.
Jeffers, E.S., Bonsall, M.B., Watson, J.E., Willis, K.J., 2012. Climate change impacts on ecosystem functioning: evidence from an Empetrum heathland. New Phytol. 193 (1), 150–164.
Juggins, S., 2016. C2 Version 1.7.7. *Software For Ecological and Palaeoecological Data Analysis and Visualisation*. Newcastle University, Newcastle upon Tyne ([Software]).
Juggins, S., 2017. Rioja: Analysis of Quaternary Science Data, R Package [Software] (http://cran.r-project.org/package=rioja, Version 0.9-15.1.
Kearney, R., Albert, P.G., Staff, R.A., Pál, I., Veres, D., Magyari, E., Ramsey, C.B., 2018. Ultra-distal fine ash occurrences of the Icelandic Askja-S Plinian eruption deposits in Southern Carpathian lakes: new age constraints on a continental scale tephrostratigraphic marker. Quat. Sci. Rev. 188, 174–182.
Kelly, T.J., Hardiman, M., Lovelady, M., Lowe, J.J., Matthews, I.P., Blockley, S.P.E., 2017. Scottish early Holocene vegetation dynamics based on pollen and tephra records from Inverlair and Loch Etteridge, Inverness-shire. Proc. Geologists' Assoc. 128 (1), 125–135.
Kim, S.T., O'Neil, J.R., 1997. Equilibrium and nonequilibrium oxygen isotope effects in synthetic carbonates. Geochem. Cosmochim. Acta 61 (16), 3461–3475.
Lane, C.S., Blockley, S.P.E., Mangerud, J., Smith, V.C., Lohne, Ø.S., Tomlinson, E.L., Matthews, I.P., Lotter, A.F., 2012. Was the 12.1 ka Icelandic Vedde Ash one of a kind? Quat. Sci. Rev. 33, 87–99.
Lang, B., Brooks, S.J., Bedford, A., Jones, R.T., Birks, H.J.B., Marshall, J.D., 2010. Regional consistency in Late-Glacial chironomid-inferred temperatures from five sites in north-west England. Quat. Sci. Rev. 29 (13), 1528–1538.
Leng, M.J., Marshall, J.D., 2004. Palaeoclimate interpretation of stable isotope data from lake sediment archives. Quat. Sci. Rev. 23 (7), 811–831.
Lotter, A.F., Eicher, U., Siegenthaler, U., Birks, H.J.B., 1992. Late-Glacial climatic oscillations as recorded in Swiss lake sediments. J. Quat. Sci. 7 (3), 187–204.
Lotter, A.F., Heiri, O., Brooks, S., van Leeuwen, J.F., Eicher, U., Ammann, B., 2012. Rapid summer temperature changes during Termination 1a: high- resolution multi-proxy climate reconstructions from Gerzensee (Switzerland). Quat. Sci. Rev. 36, 103–113.
Lowe, J.J., Walker, M.J.C., 1977. The reconstruction of the Late-Glacial environment in the southern and eastern Grampian Highlands. In: Gray, J.M., Lowe, J.J. (Eds.), Studies in the Scottish Late-Glacial Environment. Pergammon Press, Oxford, pp. 101–118.
Lowe, J., Matthews, I., Mayfield, R., Lincoln, P., Palmer, A., Staff, R., Timms, R., 2019. 'On the timing of retreat of the Loch Lomond ('Younger Dryas') readvance icefield in the SW scottish Highlands and its wider significance. Quat. Sci. Rev. 219, 171–186.
Lowe, J.J., Rasmussen, S.O., Björck, S., Hoek, W.Z., Steffensen, J.P., Walker, M.J.C., Yu, Z.C., INTIMATE Members., 2008. Synchronisation of palaeoenvironmental events in the north Atlantic region during the Last Termination: a revised protocol recommended by the INTIMATE group. Quat. Sci. Rev. 27 (1), 6–17.
MacLeod, A., Palmer, A., Lowe, J., Rose, J., Bryant, C., Merritt, J., 2011. Timing of glacier response to Younger Dryas climatic cooling in Scotland. Global Planet. Change 79 (3–4), 264–274.
Marlon, J.R., Bartlein, P.J., Walsh, M.K., Harrison, S.P., Brown, K.J., Edwards, M.E., Higuera, P.E., Power, M.J., Anderson, R.S., Briles, C., Brunelle, A., Carcaillet, C., Daniels, M., Hu, F.S., Lavoie, M., Long, C., Minckley, T., Richard, P.J.H., Scott, A.C., Shafer, D.S., Tinner, W., Umbanhowar Jr., C.E., Whitlock, C., 2009. Wildfire responses to abrupt climate change in North America. Proc. Natl. Acad. Sci. Unit. States Am. 106 (8), 2519–2524.
Marshall, J.D., Jones, R.T., Crowley, S.F., Oldfield, F., Nash, S., Bedford, A., 2002. A high resolution Late-Glacial isotopic record from Hawes Water, north-west England: climatic oscillations: calibration and comparison of palaeotemperature proxies. Palaeogeogr. Palaeoclimatol. Palaeoecol. 185 (1), 25–40.
Matthews, I.P., Birks, H.H., Bourne, A.J., Brooks, S.J., Lowe, J.J., Macleod, A., Pyne-O'Donnell, S.D.F., 2011. New age estimates and climatostratigraphic correlations for the Borrobol and penifiler tephras: evidence from Abernethy forest, Scotland. J. Quat. Sci. 26 (3), 247–252.

Mayle, F.E., Lowe, J.J., Sheldrick, C., 1997. The late devensian late-glacial palaeoenvironmental record from whitrig bog, SE Scotland. 1: lithostratigraphy, geochemistry and palaeobotany. Boreas 26 (4), 279–295.
Moore, J., 2000. Forest fire and human interaction in the early Holocene woodlands of Britain. Palaeogeogr. Palaeoclimatol. Palaeoecol. 164 (1–4), 125–137.
Moore, P.D., Webb, J.A., Collinson, M.E., 1991. Pollen Analsyis. Blackwell Scientific Publications, Oxford, p. 216pp.
Muschitiello, F., Wohlfarth, B., 2015. Time-transgressive environmental shifts across northern Europe at the onset of the younger Dryas. Quat. Sci. Rev. 109, 49–56.
Oksanen, J., Blanchet, G.F., Friendly, M., Kindt, R., Legendre, P., McGlinn, D., Minchin, P.R., O'Hara, R.B., Simpson, G.L., Solymos, P., Stevens, M.H.H., Szoecs, E., Wagner, H., 2019. Vegan: Community Ecology Package: Ordination, Diversity and Dissimilarities. CRAN [Software] Accessed 2019, Version 2.5-6. https://cran.ism.ac.jp/web/packages/vegan/vegan.pdf.
Palmer, A.P., Matthews, I.P., Lowe, J.J., MacLeod, A., Grant, R., 2020. 'A revised chronology for the growth and demise of Loch Lomond Readvance ('Younger Dryas') ice lobes in the Lochaber area, Scotland. Quat. Sci. Rev. 248, 106548.
Pennington, W., Haworth, E.Y., Bonny, A.P., Lishman, J.P., 1972. lake sediments in northern Scotland. Philosophical Transactions of the Royal Society of London, Series B, Biological Sciences 264 (861), 191–294.
Preston, C.D., Pearman, D.A., Dines, T.D., 2002. New Atlas of the British and Irish Flora. Oxford University Press, Oxford, p. 922.
Rasmussen, S.O., Andersen, K.K., Svensson, A.M., Steffensen, J.P., Vinther, B.M., Clausen, H.B., Siggaard-Andersen, M.L., Johnsen, S.J., Larsen, L.B., Dahl-Jensen, D., Bigler, M., Rothlisberger, R., Fischer, H., Gotto-Azuma, K., Hansson, M.E., Ruth, U., 2006. A new Greenland ice core chronology for the last glacial termination. J. Geophys. Res.: Atmosphere 111 (D6). https://doi.org/10.1029/2005JD006079.
Rasmussen, S.O., Bigler, M., Blockley, S.P., Blunier, T., Buchardt, S.L., Clausen, H.B., Cvijanovic, I., Dahl-Jensen, D., Johnsen, S.J., Fischer, H., Gkinis, V., Guillevic, M., Hoek, W.Z., Lowe, J.J., Pedro, J.B., Popp, T., Seierstad, I.K., Steffensen, J.P., Svenssson, A.M., Vallelonga, P., Vinther, B.M., Walker, M.J.C., Wheatley, J.J., Winstrup, M., 2014. A stratigraphic framework for abrupt climatic changes during the Last Glacial period based on three synchronized Greenland ice-core records: refining and extending the INTIMATE event stratigraphy. Quat. Sci. Rev. 106, 14–28.
Rasmussen, S.O., Vinther, B.M., Clausen, H.B., Andersen, K.K., 2007. Early Holocene climate oscillations recorded in three Greenland ice cores. Quat. Sci. Rev. 26 (15–16), 1907–1914.
Reille, M., 1992. Pollen et Spores D'Europe et D'Afrique du Nord. Laboratoire de Botanique Historique et Palynologie, Marseille, p. 520pp.
Reimer, P.J., Austin, W.E.N., Bard, E., Bayliss, A., Blackwell, P.G., Bronk Ramsey, C., Butzin, M., Cheng, H., Edwards, R.L., Friedrich, M., Grootes, P.M., Guilderson, T.P., Hajdas, I., Heaton, T.J., Hogg, A.G., Hughen, K.A., Kromer, B., Manning, S.W., Muscheler, R., Palmer, J.G., Pearson, C., van der Plicht, J., Reimer, R.W., Richards, D.A., Scott, E.M., Southon, J.R., Turney, C.S.M., Wacker, L., Adolphi, F., Büntgen, U., Capano, M., Fahrni, S.M., Fogtmann-Schulz, A., Friedrich, R., Köhler, P., Kudsk, S., Miyake, F., Olsen, J., Reinig, F., Sakamoto, M., Sookdeo, A., Talamo, S., 2020. 'The IntCal20 Northern Hemisphere radiocarbon age calibration curve (0–55 cal kBP). Radiocarbon 1–33.
Rieradevall, M., Brooks, S.J., 2001. An identification guide to subfossil Tanypodinae lar- vae (Insecta: Diptera: chironomidae) based on sephalic setation. J. Paleolimnol. 25, 81–99.
Rozanski, K., Araguas-Araguas, L., Gonfiantini, R., 1992. Relation between long-term trends of oxygen-18 isotope composition of precipitation and climate. Science 258 (5084), 981–985.
Rozanski, K., Araguás-Araguás, L., Gonfiantini, R., 1993. Isotopic patterns in modern global precipitation. In: Swart, P.K., Lohmann, K.C., McKenzie, J., Savin, S. (Eds.), Climate Change in Continental Isotopic Records. American Geophysical Union, Washington DC, pp. 1–36.
Schumacher, B.A, 2002. Methods for the Determination of Total Organic Carbon (TOC) in Soils and Sediments. United States Environmental Protection Agency, Las Vegas.
Schwander, J., Eicher, U., Ammann, B., 2000. Oxygen isotopes of lake marl at Gerzensee and Leysin (Switzerland), covering the Younger Dryas and two minor oscillations, and their correlation to the GRIP ice core. Palaeogeogr. Palaeoclimatol. Palaeoecol. 159 (3–4), 203–214.
Simpson, G.L., Birks, H.J.B., 2012. Statistical learning in palaeolimnology. In: Birks, H.J.B., Lotter, A.F., Juggins, S., Smol, J.P. (Eds.), Tracking Environmental Change Using Lake Sediments. Volume 5: Data Handling and Numerical Techniques. Kluwer Academic Publishers, Dordrecht, The Netherlands, pp. 249–327.
Simpson, G.L., Oksanen, J., 2019. Analogue and Weighted Averaging Methods for Palaeoecology. CRAN [Software] Accessed 2019, Version 0.17-3. https://cran.r-project.org/web/packages/analogue/analogue.pdf.
Stace, C., 2010. New Flora of the British Isles, third ed. Cambridge University Press, Cambridge, p. 1266pp.
Steffensen, J.P., Andersen, K.K., Bigler, M., Clausen, H.B., Dahl-Jensen, D., Fischer, H., Goto-Azuma, K., Hansson, M., Johnsen, S.J., Jouzel, J., Masson-Delmotte, V., Popp, T., Rasmussen, S.O., Rothlisberger, R., Ruth, R., Stauffer, B., Siggaard-Andersen, M.L., Sveinbjornsdottir, A.E., Svensson, A., White, J.W., 2008. High-resolution Greenland ice-core data show abrupt climate change happens in few years. Science 321 (5889), 680–684.
Talbot, M.R., 1990. A review of the palaeohydrological interpretation of carbon and oxygen isotopic ratios in primary lacustrine carbonates. Chem. Geol. Isot. Geosci. 80 (4), 261–279.
Tarasov, L., Peltier, W.R., 2005. Arctic freshwater forcing of the Younger Dryas cold reversal. Nature 435 (7042), 662.
ter Braak, C.J.F., Juggins, S., 1993. Weighted averaging partial least squares regression (WA-PLS): an improved method for reconstructing environmental variables from species assemblages. Hydrobiol. (Sofia) 269 (270), 485–502.
Thomas, P.A., El-Barghathi, M., Polwart, A., 2007. Biological flora of the British Isles: Juniperus communis L. J. Ecol. 95 (6), 1404–1440.
Thornalley, D.J., McCave, I.N., Elderfield, H., 2010. Freshwater input and abrupt deglacial climate change in the North Atlantic. Paleoceanography 25 (1).
Timms, R.G.O., Matthews, I.P., Lowe, J.J., Palmer, A.P., Weston, D.J., MacLeod, A., Blockley, S.P.E., 2019. Establishing tephrostratigraphic frameworks to aid the study of abrupt climatic and glacial transitions: a case study of the Last Glacial-Interglacial Transition in the British Isles (c. 16-8 ka BP). Earth Sci. Rev. 192, 34–64.
Timms, R.G.O., Matthews, I.P., Palmer, A.P., Candy, I., Abel, L., 2017. A high-resolution tephrostratigraphy from quoyloo meadow, orkney, Scotland: implications for the tephrostratigraphy of NW Europe during the last glacial-interglacial transition. Quat. Geochronol. 40, 67–81.
Turner, J.N., Holmes, N., Davis, S.R., Leng, M.J., Langdon, C., Scaife, R.G., 2015. 'A multiproxy (micro-XRF, pollen, chironomid and stable isotope) lake sediment record for the Lateglacial to Holocene transition from Thomastown Bog, Ireland. J. Quat. Sci. 30 (6), 514–528.
Turney, C.S.M., Harkness, D.D., Lowe, J.J., 1997. The use of microtephra horizons to correlate Late-glacial lake sediment successions in Scotland. J. Quat. Sci. 12 (6), 525–531.
van Asch, N., Hoek, W.Z., 2012. The impact of summer temperature changes on vegetation development in Ireland during the Weichselian Lateglacial Interstadial. J. Quat. Sci. 27 (5), 441–450.
van Asch, N., Lutz, A.F., Duijkers, M.C., Heiri, O., Brooks, S.J., Hoek, W.Z., 2012. Rapid climate change during the Weichselian Late-Glacial in Ireland: chironomid-inferred summer temperatures from Fiddaun. Co. Galway.' *Palaeogeography, Palaeoclimatology, Palaeoecology* 315–316, 1–11.
van Dinter, M., Birks, H.H., 1996. Distinguishing fossil *Betula nana* and *B. pubescens* using their wingless fruits: implications for the late-glacial vegetational history of western Norway. Veg. Hist. Archaeobotany 5 (3), 229–240.
van Raden, U.J., Colombaroli, D., Gilli, A., Schwander, J., Bernasconi, S.M., van Leeuwen, J., Leuenberger, M., Eicher, U., 2013. High-resolution late-glacial chronology for the Gerzensee lake record (Switzerland): $\delta^{18}O$ correlation between a Gerzensee-stack and NGRIP. Palaeogeogr. Palaeoclimatol. Palaeoecol. 391, 13–24.
von Grafenstein, U., Erlenkeuser, H., Brauer, A., Jouzel, J., Johnsen, S.J., 1999. A mid-European decadal isotope-climate record from 15,500 to 5000 years BP. Science 284 (5420), 1654–1657.
Walker, M.J.C., 1975. Late-glacial and early post-glacial environmental history of the central grampian Highlands, Scotland. J. Biogeogr. 2 (4), 265–284.
Walker, M.J.C., Lowe, J.J., 1990. Reconstructing the environmental history of the last glacial-interglacial transition: evidence from the Isle of Skye, inner hebrides, Scotland. Quat. Sci. Rev. 9 (1), 15–49.
Walker, M.J.C., Lowe, J.J., 2017. Lateglacial Environmental Change in Scotland.' Earth and Environmental Science Transactions of the Royal Society of Edinburgh, pp. 1–26.
Walker, M., Lowe, J., Blockley, S.P., Bryant, C., Coombes, P., Davies, S., Hardiman, M., Turney, C.S., Watson, J., 2012. 'Lateglacial and early Holocene palaeoenvironmental 'events' in Sluggan Bog, Northern Ireland: comparisons with the Greenland NGRIP GICC05 event stratigraphy. Quat. Sci. Rev. 36, 124–138.
Watson, J., 2008. Quantifying Late Glacial Climate Change in Northwestern Europe Using Two Insect Proxies. Unpublished PhD Thesis. Queens University Belfast, p. 365.
Wiederholm, T. (Ed.), 1983. Chironomidae of the Holarctic Region. Keys and Diagnoses. Part I. Larvae, vol. 19. Entomologica Scandinavia Supplement, pp. 1–457.
Whittington, G., Edwards, K.J., Zanchetta, G., Keen, D.H., Bunting, M.J., Fallick, A.E., Bryant, C.L., 2015. Lateglacial and early Holocene climates of the Atlantic margins of Europe: stable isotope, mollusc and pollen records from Orkney, Scotland. Quat. Sci. Rev. 122, 112–130.
Wohlfarth, B., Blaauw, M., Davies, S.M., Andersson, M., Wastegård, S., Hormes, A., Possnert, G., 2006. Constraining the age of Lateglacial and early Holocene pollen zones and tephra horizons in southern Sweden with Bayesian probability methods. J. Quat. Sci. 21 (4), 321–334.
Wohlfarth, B., Muschitiello, F., Greenwood, S.L., Andersson, A., Kylander, M., Smittenberg, R.H., Steinthorsdottir, M., Watson, J., Whitehouse, N.J., 2017. 'Hässeldala–a key site for Last Termination climate events in northern Europe. Boreas 46 (2), 143–161.